THE FORMATION OF LOW MASS STARS

An Observational Overview

CHARLES J. LADA
Smithsonian Astrophysical Observatory
60 Garden Street
Cambridge, MA 02138 USA

1. Introduction: The Continuing Process of Star Formation

The question of the origin of stars is one of the most fundamental of astronomy. Yet, despite thousands of years of stellar observation, and early speculations by Newton and Laplace, it has only been in the latter part of the present century that the investigation of star formation has become an active discipline of astrophysical research. That the origin of stars has remained so mysterious for so long is largely due to the fact that the process of star formation has never been directly observed either with the naked eye or the with most powerful telescopes. Moreover, prior to the twentieth century neither the energy source nor the bulk composition of stars were known. Indeed, without knowledge of the physical nature of stars it was very difficult to develop an understanding of their origin. At the end of the nineteenth century, the nature of the mystery surrounding stellar origins was nicely summed up by the fictional character Huck Finn (in the book The Adventures of Huck Finn by Mark Twain) when he observed the stars in the night sky and wondered "*...did they just happen or was they made?*"

Have the stars been around since creation or were they being made in the heavens? As far as anybody could tell at dawn of this century, the entire universe consisted of a single stellar system, stars lived forever and the question of the origin of stars was a question of cosmology. As such the problem of star formation was not susceptible to detailed scientific investigation. That is, even the most basic hypotheses concerning stellar origins could not be directly tested by observation. Fortunately, over the last half century astronomical research has lead to the fundamental realization that star formation has been a continuous, ongoing process throughout the history of the Galaxy and the universe. This critical fact has been demonstrated by both theory and observation.

Perhaps the most important step contributing to this realization was the discovery of the nature of stars as natural thermonuclear reactors which fuse hydrogen, the primary product of the Big Bang, into helium and then ultimately into the heavier elements which make up the periodic table. This process is elegantly explained by the theory of stellar structure and evolution, perhaps the greatest theoretical achievement of twentieth century astronomy. Although this great theory does not in any way account for or predict the formation of stars (and is in this sense incomplete), it has successfully explained the basic physical properties of stars as well as the processes of stellar evolution and death once stars exhaust their nuclear fuel reserves. In particular, stellar evolution theory demonstrated that certain luminous stars, OB stars, burn their nuclear fuel at such prodigious rates that they can live for only a small fraction of the lifetime of our galaxy. The existence of such stars clearly indicates that star formation has occured in the present epoch of Galactic history.

The relative youth of OB stars was also clearly demonstrated by observations of their spatial distribution on the sky. In 1947 the Armenian astronomer V.A. Armbartsumian showed that OB stars were almost always members of stellar groupings he termed OB Associations. Furthermore he found that the space densities of stars in OB associations were well below the threshold necessary to prevent their disruption by Galactic tidal forces. Ambartsumian calculated dynamical ages for the associations that were much less than the age of the galaxy. These dynamical ages turned out to be in good agreement with the nuclear ages of the stars and independently provided evidence that star formation is still an active process in the Galaxy.

The discovery of the interstellar medium of gas and dust during the early part of the twentieth century provided a crucial piece of corroborating evidence in support of the concept of present epoch Galactic star formation. Subsequent observations of interstellar material established that clouds of interstellar gas and dust had roughly stellar composition and were considerably more massive than a single star or group of stars. This revealed that the raw material to make new stars was relatively abundant in the Galaxy. These three pieces of evidence, 1) stellar evolution theory, 2) expanding OB associations and 3) the interstellar medium, constitute three basic "proofs" of ongoing star formation in the Milky Way.

Because star formation is occurring in the present epoch, the question of the origin of stars can be investigated by direct observation. If this were not the case, the prospects for completing the theory of stellar structure and evolution with a description of how stars form would be bleak. Yet, for most of the century, direct observation of the star formation process and the development of a theory to explain it, were severely hampered by the fact that most stars form in dark clouds and during their formative stages are invisible optically. Fortunately, advances in observational technology over the last quarter century opened the infrared and millimeter-wave windows to astronomical investigation and enabled direct observations of star forming regions and this has significantly expanded our knowledge of the star formation process. As a result the foundations for a coherent theory of star formation and early evolution are being laid.

In this chapter I will attempt to present a general overview of the critical observations which form the basis of our current understanding of the origins of low mass, sunlike, stars. The present review significantly updates earlier treatments of this topic which I wrote for the first Crete volume [71] and later the Proceedings of the Seventh Guo Shoujing Summer School on Astrophysics [135].

2. Stellar Observations: The Fossil Record

2.1. ASSOCIATIONS AND CLUSTERS

Stars in the disk of our galaxy can be categorized by their spatial distribution as being either members of the general Galactic field population or members of associations or clusters. An association or cluster is defined as a group of stars of the same physical type whose surface density significantly exceeds that of the field for stars of the same physical type [72]. Associations differ from clusters in their space densities: associations have space densities well below that (i.e., 0.1 $M_{\odot}$ pc^{-1}) [21] required for stability against galactic tides while clusters have space densities (e.g., $\geq$ 1.0 $M_{\odot}$ pc^{-1}) considerably in excess of the tidal stability limit. The spatial extents of associations are typically very large, 50 - 150 parsecs, while clusters are typically small in size ($\approx$ 1 parsec in diameter). Only a very small fraction of the stars in the disk of the Galaxy are presently members of associations or clusters. However, virtually all known O stars are members of OB associations. This indicates that all O stars formed in OB associations and results from the fact that the dynamical ages of OB associations (i.e., approximately 10^7 years) are greater than the lifetimes of the individual O stars ($\sim 10^6$ yrs.). About 10% of all B stars are members of associations. But when one takes into account that the lifetime of a B star is an order of magnitude larger than the lifetime of an association, it is clear that all present day B stars probably formed in OB associations. [18, **?**]

OB associations contain considerably more low mass stars than OB stars, but the spatial density of these fainter stars is not that much greater than that of faint field stars. Consequently, the low mass component of OB associations is very difficult to identify from stellar density counts alone. If a stellar association is sufficiently young ($\leq 2 - 3$x10^6 yrs.) then many of its low mass stars are likely to be emission-line (T Tauri type) stars. Emission-line stars are relatively rare in the field and groups of young, low mass T-Tauri stars can be easily identified as T associations, even if their surface densities are relatively low. In most instances T associations spatially coexist with OB associations [35] and trace the low mass component of such stellar groups. As will be discussed later, observations of very young associations (those embedded in molecular clouds) suggest the ratio of OB stars to low mass stars is roughly given by the initial mass function for local field stars. Consequently, it follows that OB associations can account for the formation of nearly all stars being born in the present epoch of galactic history. However, it is interesting to note that if OB associations were producing stars over the age of the Galaxy at the rate currently observed they would account for only about 10% of the stellar mass of the Milky Way. Open clusters are stellar systems which are stable against galactic tides and have considerably longer lifetimes (10^8 yrs.) than associations. Roughly 10% of all stars being formed end up as members of bound open clusters [109]. However most open clusters themselves probably formed inside OB associations.

The internal radial velocity dispersions of OB association members are typically on the order of 2-3 $\mathrm{km\,s^{-1}}$. It is important to bear in mind that even in the absence of galactic tidal forces, these motions are too large to allow the associations to be bound by self-gravity. It has long been recognized that OB associations could provide important information about the star formation process since they are so young that the individual members have not had enough time to move very far from their places of birth. For example, the present sizes of OB associations must closely reflect the sizes of the clouds which spawned them [18, 34, 35]. In addition, the structure of OB associations can provide important fossil clues about the structure and even the temporal evolution of a star forming complex. One common property of OB associations is that they are sub-structured, often consisting of sub-groupings of sequentially differing age [17]. Such sub-structure has suggested that star formation proceeds through a star forming region in an ordered temporal sequence. The chain reaction like nature of the spatial-temporal structure of OB subgroups has lead to the suggestion that OB subgroups are formed by a process of sequential triggering [35].

2.2. MULTIPLICITY

The tendency for stars to form in groups is not limited to associations and clusters. On much smaller, more intimate size scales (i.e., 1-100 AU) we find that most stars are members of binary or multiple star systems. For example, radial velocity measurements of field G dwarf stars indicate that

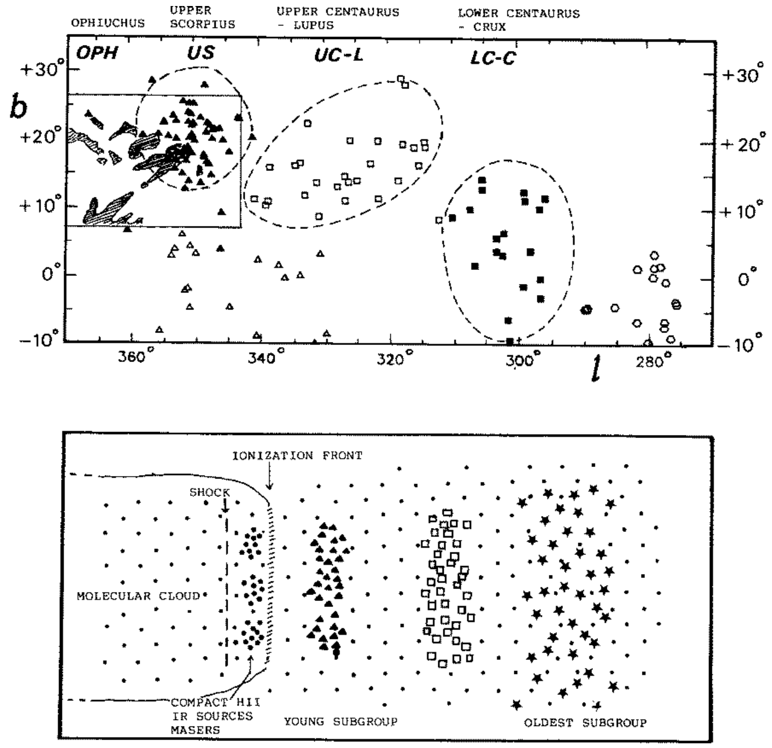

Figure 1. *(Top) Positions of OB stars in the Oph-Sco-Cen Association. The subgroups are outlined and a sketch of the dark clouds in the Ophiuchus region is also shown. (Bottom) A schematic diagram illustrating the Elmegreen-Lada sequentially triggered star formation model for OB subgroups. Figure adapted from Blaauw (1991).*

roughly 57% of all such stars have stellar companions [1, 32]. The binarity fraction does not appear to depend too strongly on spectral type as studies of both M dwarfs [38] and B stars [126] have indicated. Since some binaries may have been disrupted since formation, these fractions could be lower limits to the actual fraction of binary stars produced in the star formation process. Binary stars provide a strong constraint for star formation theories. In this regard, it is interesting to note that the mass of binary companions seems to be independent of the mass of their primaries [32].

2.3. THE INITIAL MASS FUNCTION

A fundamental consequence of the theory of stellar evolution is that the life history of a star is almost entirely pre-determined by its initial mass.

Consequently, to understand star formation and the consequent luminosity evolution of the galaxy requires a detailed knowledge of both the initial distribution of stellar masses at birth and how this quantity varies through space and time within the galaxy. Unfortunately, stellar evolution theory is not able to predict the Initial Mass Function (IMF) of stars. This quantity must be derived from observations. However, to do so is not straightforward because stellar mass is not itself an observable quantity. Stellar radiant flux or luminosity is the most readily observed property of a star. Therefore, the starting point of any attempt to determine a stellar mass spectrum is the determination of a stellar luminosity function. Then, an appropriate mass-luminosity relation is required to transform the luminosity function into a stellar mass function.

The first attempt to derive an empirical initial mass spectrum was carried out by Salpeter [111] who used as a starting point the general (or van Rhijn) luminosity function determined for field stars within the neighborhood of the sun. The field star luminosity function, $\Phi(M_V)$, is the relative number of stars per unit magnitude interval per unit volume of space as a function of absolute magnitude, M_V, in the solar neighborhood. (The determination of the field star luminosity function is itself a difficult task and discussion of this is beyond the scope of this chapter, and the reader who desires more information on this topic is referred to the text by Mihalas and Binney [94]). In principle, the field star luminosity function counts all presently visible field stars in the neighborhood of the sun. Because stars more massive than the sun have main sequence lifetimes shorter than that of the galaxy they are under represented in the field star luminosity function with respect to low mass stars, whose lifetimes are in excess of the age of the galaxy. Therefore, the present day field star luminosity function is biased toward low luminosity stars and must be corrected for the effects of post–main–sequence stellar evolution to obtain a luminosity function more representative of that produced at stellar birth.

Salpeter introduced the concept of an initial luminosity function, $\Psi(M_V)$, which is the relative number of stars per unit volume in each absolute magnitude interval originally produced by the star formation process. He derived $\Psi(M_V)$ from the field star luminosity function as follows:

$$\Psi(M_V) = \Phi(M_V) \quad for \quad \tau_{MS} \geq \tau_{MW}$$

and

$$\Psi(M_V) = \frac{\tau_{MW}}{\tau_{MS}}\Phi(M_V) \quad for \quad \tau_{MS} < \tau_{MW}$$

where τ_{MW} is the age of the galaxy and τ_{MS} is the main sequence lifetime of a star under consideration. Here, it has been assumed for simplicity that the stellar birthrate and the form of $\Psi(M_V)$ has been constant with time over the age of the galaxy. To derive an initial distribution of stellar mass we need to apply a mass luminosity relation to $\Psi(M_V)$. With the additional assumption that $\Psi(M_V)$ counts only main sequence stars, we can use the empirical mass-luminosity relation for main sequence stars (i.e., $L_* \sim m_*^p$, where $p \approx 3.45$) [116, 5]. Because $\Psi(M_V)$ is a distribution of stellar (absolute, visual) magnitudes and not luminosities, it is convenient to use a form of the mass-luminosity relation that relates M_V to stellar mass. Since $L_* \sim m_*^p$, and $M_V \sim \log L_*$, then $M_V \sim \log m_*$. Consequently it is useful to introduce the concept of the initial mass function $\xi(logm)$ which is the relative number of stars formed per unit volume per unit *logarithmic* mass interval and is straightforwardly related to $\Psi(M_V)$ as follows:

$$\Psi(M_V)dM_V = \xi(logm_*)dlogm_*.$$

The shape of the initial mass function is usually characterized by a spectral index, $\beta \equiv \partial log\xi(logm_*)/\partial logm_*$, which is the slope of the function in a log-log plot. We note that the initial mass *spectrum*, $f(m_*)$, (i.e., the differential frequency distribution of stellar masses at birth) is related to the mass function by:

$$\xi(logm_*) = \frac{m_* f(m_*)}{0.434}.$$

The spectral index of the mass spectrum, γ, is equal to $\beta - 1$.

Salpeter found that the initial mass function (IMF) could be reasonably well represented by a simple power-law form viz:

$$\xi(logm_*) \sim m_*^{-1.35}$$

In other words, a constant spectral index over the range of stellar mass that was considered, between approximately 0.4 and 10 $M_\odot$. In addition, the value of the spectral index (being less than -1.0) indicated that more stellar mass was contained in low mass stars than in high mass stars.

However, more recent and detailed studies [113, 65, 66, 115] suggest that the field star IMF is not characterized by a single spectral index. In particular, at masses around 1 $M_\odot$, there is a break in the power-law slope and the IMF becomes flatter at lower masses (i.e., $\xi(logm_*) \sim m_*^{-0.2}$). The presence of such a break in the IMF is significant and suggests that there may be a characteristic mass of star formation of around a solar mass or even less. However, it is not clear whether the IMF remains flat or decreases at the lowest masses. In fact, for stellar masses near and below the hydrogen burning limit (i.e. ≤ 0.08 $M_\odot$, the brown dwarf regieme) the IMF is very poorly constrained by existing observations. In any event, it is still clear that most stars that form in the galaxy are low mass objects.

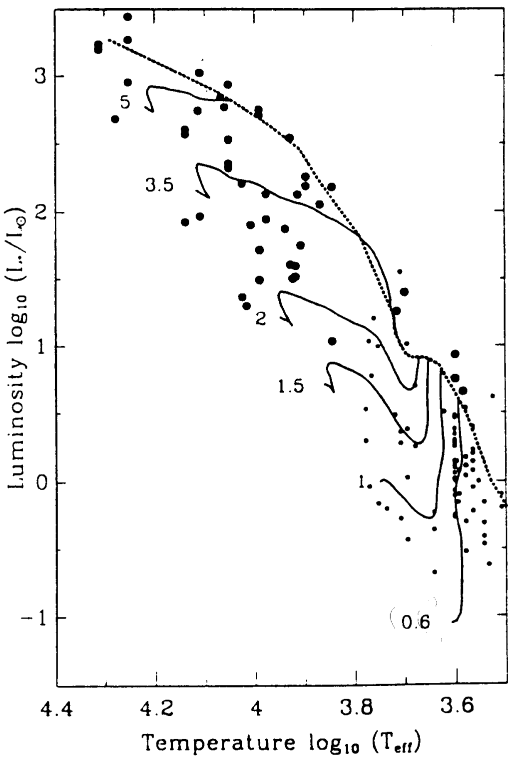

Figure 2. *The HR diagram for a selection of pre-main sequence stars taken from a paper by Palla and Stahler (1993). Theoretical tracks (solid curves) for selected stellar masses are shown along with the birthline (dotted curve).*

2.4. THE HR DIAGRAM AND EARLY STELLAR EVOLUTION

The HR diagram is a very powerful tool for studying stellar evolution. Throughout most of its life a star will appear on the main sequence (the locus of positions in the HR diagram for stable hydrogen burning stars). The location of a star on the main sequence is determined almost solely by its mass. The main sequence lifetime of a star is also a very strong function of its mass. The more massive a star the shorter its main sequence lifetime. The utility of the HR diagram for investigating stellar evolution is best illustrated by its application to stellar clusters. In particular, the locations of cluster stars in the HR diagram with respect to the main sequence are determined primarily by the age of the cluster. For example, nearly 40 years ago a photometric study of the young cluster NGC 2264 by Walker [128] showed that most of the stars in this group, specifically all stars with spectral types later than about A0, were characterized by luminosities and effective temperatures which placed them above the main sequence in the subgiant region of the HR diagram (just below the locations one would expect to find red giants and long period variables). That the more massive stars with earlier spectral types were found to be on the main sequence strongly suggested that the population of subgiant stars in this cluster were pre-main sequence stars rather than post-main sequence stars. That is, these stars were not yet hydrogen burning objects. Many of these pre-main sequence stars turned out to be emission-line, T-Tauri type stars. This observation thus provided strong confirming evidence in support of the notion that T associations are very young.

Stellar evolution theory predicts that pre-hydrogen burning stars will lie above the main sequence and describes in detail the early evolution of such stars in the HR diagram. Figure 3 shows the HR diagram for a selection of pre-main sequence stars with masses between roughly 0.5-5 $M_\odot$ [103]. These pre-main sequence stars form a band stretching across the HR diagram parallel the main sequence which forms it lower boundary. The fact that this band has a distinct upper envelope is very significant. This upper boundary, termed the "birthline" [120], marks the positions of young stars when they first appear on the HR diagram. For a star of a given mass this position corresponds to a specific size or stellar radius. In other words, a star first becomes observable and appears on the HR diagram only after it obtains a specific maximum size, evidently pre-determined by its prior protostellar evolution. The birthline represents the initial condition for pre-main sequence (quasi-static) contraction. It is the dividing line between the protostellar and pre-main sequence stages of stellar evolution. Stellar evolution theory does not predict the existence of the birthline. Indeed, when evolving off the main sequence a star will expand to a size well beyond its birthline position. The physics which determine the birthline are the mysterious physics of protostellar evolution. Understanding the nature of protostars is, at present, the major frontier of star formation research.

Once a star reaches the birthline its subsequent evolution in the HR diagram depends on its mass. The theoretical evolutionary trajectories or tracks of 6 stars ranging in mass from 0.6 $M_\odot$ to 5 $M_\odot$ are plotted in Figure 3. Low mass stars start out as fully convective stars and descend to the main sequence along nearly vertical trajectories or convective tracks [51]. The lowest mass stars remain fully convective until they reach the main sequence. Stars with masses of about 0.8 $M_\odot$ or greater develop radiative interiors before reaching the main sequence. That is, the conditions in the interiors of these stars make it easier for them to transport energy outward by radiation than convection. According to the theory, once a star is radiative its luminosity is primarily dependent on its mass. This holds for any radiative star whether or not it is on the main sequence or is a post-or pre-main sequence object. Thus, such radiative stars evolve to (or away from) the main sequence with roughly constant luminosity on more or less horizontal (radiative) tracks on the HR diagram [55]. Stars with masses greater than about 3 $M_\odot$ miss the (pre-main sequence) convective phase altogether. Pre-main sequence evolutionary tracks are useful not only for determining the masses of pre-main sequence stars but also for determining their ages *subsequent to their appearance on the birthline.* Prior to their appearing on the birthline, stars are in the protostellar stage of evolution and for reasons to be discussed later cannot be easily placed in the HR diagram. Finally, we point out that only low mass stars are expected to have a pre-main sequence phase of evolution. This is illustrated by the fact that the birthline intersects the main sequence for stars of roughly 8 $M_\odot$. Stars more massive than this begin to burn hydrogen and reach the main sequence before their protostellar stage of evolution ends. The physical reason for this becomes apparent if one compares the timescale for pre-main sequence evolution with that of protostellar collapse. The timescale for the gravitational collapse of a cloud core, the free-fall time, is determined largely by ρ, the density of the cloud:

$$\tau_{ff} = \sqrt{\frac{3\pi}{32G\rho}}$$

For the typical mean density (n $\approx 10^4$ cm^{-3}) of a cloud core (of either low or high mass) the free–fall time is about 4 x 10^5 years. The time scale for pre-hydrogen burning evolution is the Kelvin-Helmotz time:

$$\tau_{KH} \approx \frac{GM_*^2}{R_* L_*}$$

which is very rapid for a high mass star (i.e., $\approx 10^4$ years for $M_* = 50\ M_\odot$) and relatively slow for a low mass star (i.e., $\approx 3 \mathrm{x} 10^7$ years for $M_* = 1\ M_\odot$). More importantly for high mass stars $\tau_{KH} < \tau_{ff}$ and these stars begin burning hydrogen and reach the main sequence before the termination of the infall or collapse phase of protostellar evolution. On the other hand, for low mass stars $\tau_{KH} > \tau_{ff}$ and low mass stars have an *observable* pre-main sequence stage of stellar evolution.

3. Giant Molecular Clouds: Sites Star Formation

3.1. OB ASSOCIATIONS AND GMCS

As mentioned earlier, stars in OB associations are still very near the locations where they were born. It is therefore not surprising that OB associations are invariably associated with visible manifestations of interstellar gas

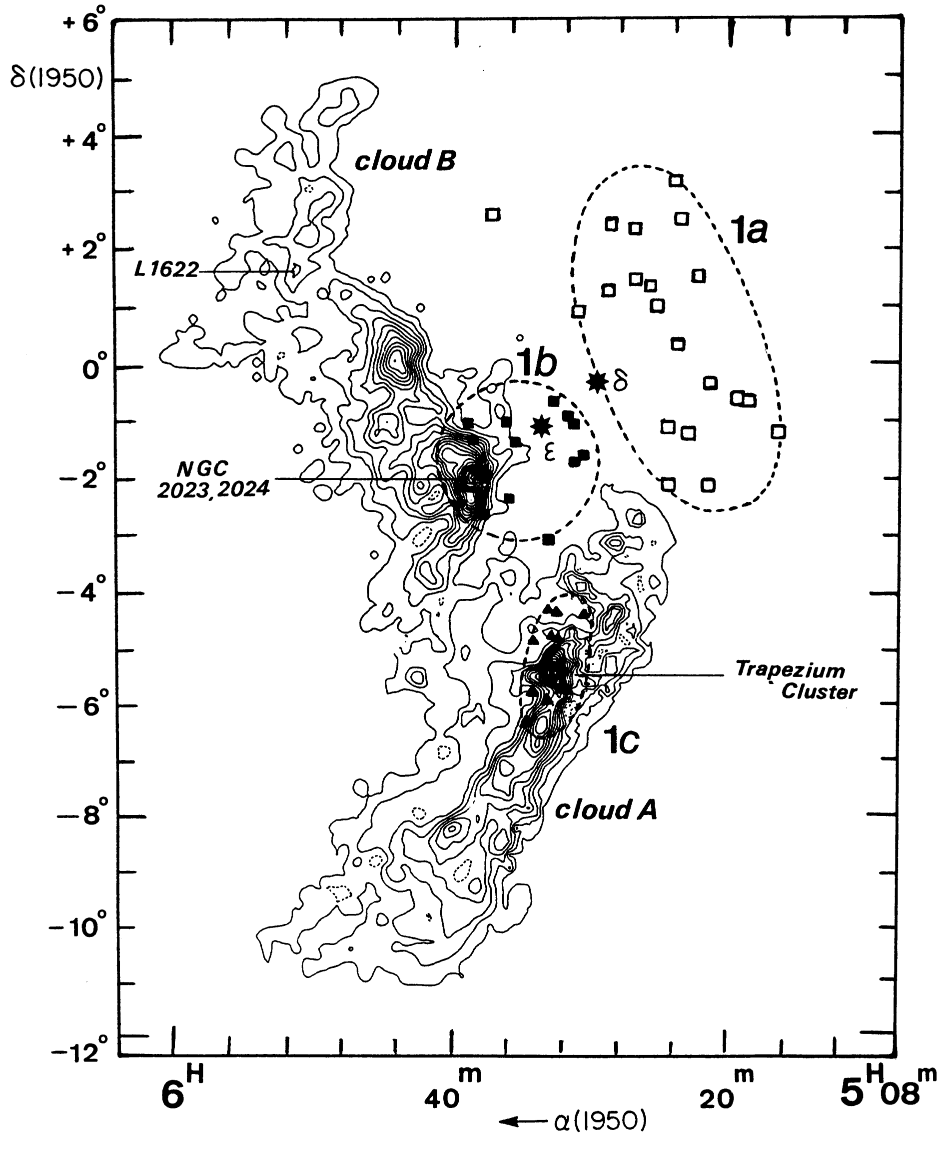

Figure 3. The ORI OB1 association and its Giant Molecular Cloud Complex. The 4 subgroups of sequentially differing age are enclosed by dashed lines. The oldest (1a) is significantly more expanded than the youngest (Trapezium Cluster). Figure taken from Blaauw (1991).

and dust [17]. In particular, virtually all known OB associations are spatially associated with Giant Molecular Clouds [34, 35, 19]. A good example of this is shown in Figure 3 which plots the positions of the OB subgroups in the Ori I association along with a map of the Orion GMC. The Orion region illustrates three important properties of OB associations and their associated GMCs: 1) The dimensions of the GMC are comparable to if not larger than those of the OB association. 2) The OB subgroups differ in size and age with the youngest (in this case the Trapezium cluster) usually the smallest and often exciting an HII region (in this case the famous Orion Nebula) or reflection nebula and therefore demonstrating a direct *physical* relation to the GMC. 3) The mass of the GMC ($\approx 2 - 3\mathrm{x}10^5 \mathrm{M}_\odot$) is considerably larger than that of the OB association ($\approx 10^3$ $\mathrm{M}_\odot$). From these three considerations it follows that that OB associations, and consequently most all stars currently forming in the galaxy, are born in GMCs.

The large difference between the stellar mass of the OB association and the molecular cloud (3) illustrates a fundamental property of star formation in GMCs. Namely, that the star formation efficiency (SFE=stellar mass/(stellar + gaseous mass)) in GMCs is low. For example, in the λ Ori OB association a direct comparison of the stellar and molecular mass of the star forming complex yielded an observed efficiency of only 0.3 % [31]. Although this is probably a lower limit to the true efficiency, it likely falls short by no more than a factor of 5. Thus we expect typical SFEs of at most a few % in GMCs which when combined with the estimates of 10^9 $\mathrm{M}_\odot$ for the total mass of GMCs in the Galaxy, and 10^7 yrs. for the typical lifetimes of GMCs, results in a star formation rate that is consistent with the overall rate for the galaxy of roughly 2-3 $\mathrm{M}_\odot$ yr^{-1}, derived from other observations [138].

The low efficiency of star formation in GMCs is of central importance for understanding the dynamical nature of OB associations. The unbound state of stellar associations is a natural consequence of star formation with a low conversion efficiency of gas to stars followed by a rapid removal of the unprocessed gas from the system [31, 68]. Figure 4 is a schematic sketch which depicts the evolution of star formation in a GMC and the creation of an expanding association [68]. First, low mass stars form in dense cores located throughout the cloud converting roughly 1-3% of the total gaseous mass into stars. At some point massive O stars form in the cloud and heat, ionize and disrupt the molecular gas. (We note here that it is not clear at the present time whether most of the low mass stars are formed prior to the O stars or whether the episode of O star formation is also accompanied by an increase in the production of low mass stars.) In a relatively short time ($\approx 10^6$ years), the O stars disrupt the entire complex and remove the vast majority of the original binding mass of the system. (Calculations show that O stars can disrupt an entire GMC if only 4% of the total cloud mass is converted into stars with a normal IMF [131].) The stars in the cloud, which were originally orbiting in virial equilibrium with the deep potential

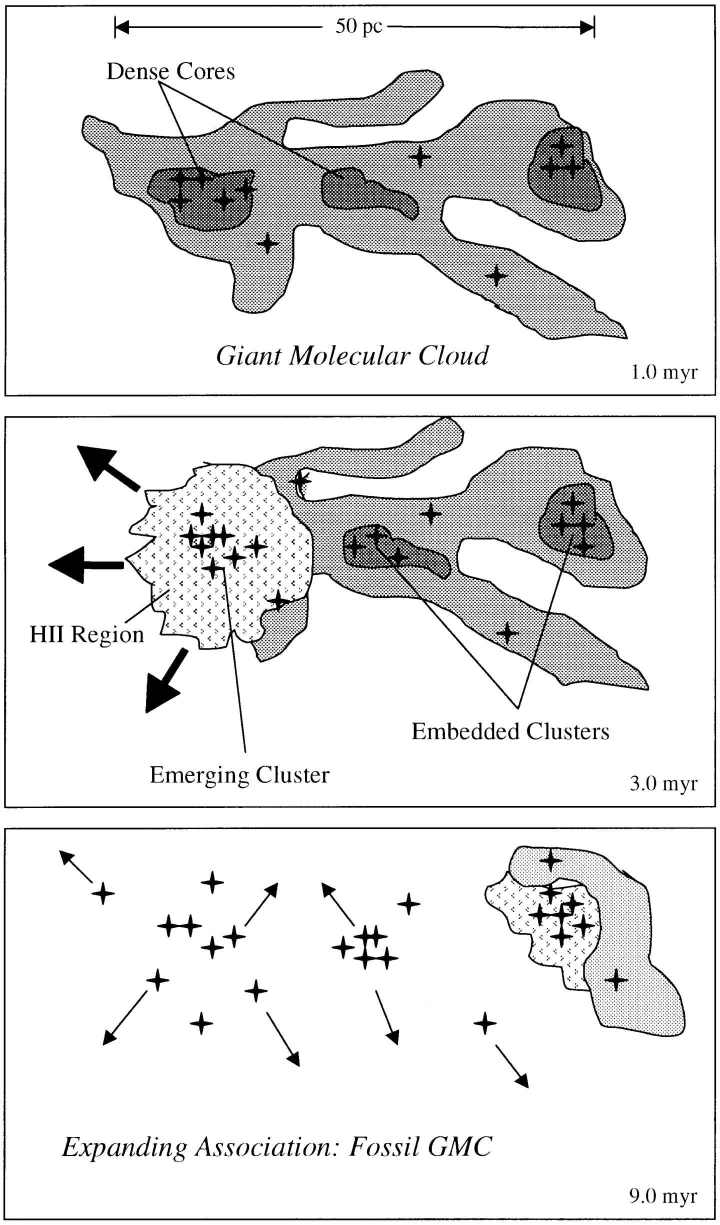

Figure 4. *A schematic diagram illustrating the evolution of an OB association.*

well of the massive GMC, respond to the rapid removal of the majority of the binding mass by freely expanding into space with their initial virial velocities. This hypothesis predicts that the velocity dispersion of stars in an OB association should be on the same order of that of the molecular gas in a GMC (i.e., 2-4 $\mathrm{km\,s^{-1}}$) which agrees with observations as discussed earlier [18]. In addition it is interesting to note that the angular sizes of OB subgroups within an association increase with age of the subgroup in a manner which is consistent with typical expansion velocities (of about 2 $\mathrm{km\,s^{-1}}$)[17, 18] (see also Figure 3). The very few associations that are not near a GMC, such as Cas-Tau or Lac OB1 are associated with smaller molecular clouds and moreover have ages of $\approx$ 20 million years, making them among the oldest OB associations known [18]. They have probably existed long enough to have completely disrupted their parental GMCs.

With sizes on the order of 100 pc GMCs are the largest known objects in the Galaxy. Moreover, with masses in excess of 10^5 $\mathrm{M_\odot}$, GMCs rival globular clusters as the most massive objects in the Milky Way. Molecular clouds are characterized by gas kinetic temperatures in the range between 10-50 K making them the coldest objects in the universe. There are a few thousand GMCs in the Galaxy and they account for a substantial fraction of all interstellar matter. Giant molecular clouds are composed primarily of hydrogen which is mostly molecular in form due to the low temperatures which characterize the gas. However, two factors make molecular hydrogen generally unobservable in molecular clouds: first, because it is a homonuclear molecule molecular hydrogen lacks a permanent dipole moment and its rotational transitions are extraordinarily weak; second, it is so light in weight that its lowest rotational transitions are at mid-infrared wavelengths and are too energetic to be collisionally excited at the temperatures that characterize GMCs. Consequently GMCs are best traced by emission lines of molecules such as CO, CS or NH_3 and much of what we know about the physical conditions in GMCs is derived from observations of these molecules.

3.2. PHYSICAL PROPERTIES OF GMCS

Molecular emission lines from GMCs are typically characterized by linewidths in the range 2-4 $\mathrm{km\,s^{-1}}$. Given the masses and sizes of these clouds, their linewidths are close to what one would predict if the clouds are in virial equilibrium, (i.e., $\Delta V \approx (GM/R)^{-0.5}$) which is consistent with the idea that the clouds are bound. At the same time however, the linewidths are considerably greater than that expected for thermal motion

Physical Properties of A Standard GMC	
Mass	$2-3\times10^{5}$ $M_\odot$
Maximum Linear Extent	50-100 pc
Mean Density(n(H_2))	200-300 cm^{-3}
Mean N(H_2)	$3-6\times10^{21}$ cm^{-2}
Typical Linewidth	2-4 $km\,s^{-1}$
Kinetic Temperature	10 K
Sound Speed	0.2 $km\,s^{-1}$
Typical Magnetic Field Strength	30 μG
Alfven Speed	3 $km\,s^{-1}$

of the emitting gas molecules (of mass m):

$$\Delta V_{FWHP} = 2.354(kT/m)^{0.5} = 0.05\ kms^{-1} \text{ for CO.}$$

This indicates that the overall dynamical state of a GMC is characterized by supersonic, non-thermal, bulk motions. If these motions are turbulent in nature, they should be highly dissipative, [42] yet GMCs maintain their supersonic dynamical states throughout their lifetimes, estimated to be on the order of 10^7 to 10^8 years. Although they are gravitationally bound, GMCs cannot be in a state of overall dynamical collapse because the resulting star formation rate (~ 250 $M_\odot$ yr^{-1}) would be considerably in excess of observed values [138]. Moreover, the free-fall time for the collapse of a GMC is short compared to the its lifetime. Therefore it is clear that GMCs are being supported against global dynamical collapse by some mechanism. However, GMCs are too cold to be supported by thermal pressure. Exactly what does support GMCs against collapse has been a long standing problem in star formation research.

Molecular clouds are permeated by magnetic fields with strengths in the range of 10 to 1000 μG [53]. The largest values arise in extremely dense, very compact regions which exhibit OH maser emission. More typical field strengths are on the order of about 30 μG. The Alfven speed, $v_A = B/(4\pi\rho)^{\frac{1}{2}}$ is therefore about 3 $km s^{-1}$. Thus the fluid motions within a GMC are sub-Alfvenic and perhaps less dissipative than is suggested by their otherwise supersonic dynamical state. Moreover these field strengths are sufficiently strong that they may retard or prevent the global collapse of a GMC [96, 97]. The typical physical properties of GMCs in the solar neighborhood are summarized in Table 1

3.3. THE STRUCTURE OF GMCS: DENSE CORES

The molecular mass of a GMC is spatially distributed in a non-uniform manner. These clouds are highly structured, consisting of numerous filaments, clumps and dense cores [20]. In fact GMCs are so complex that it is very difficult to provide a meaningful quantitative description of their structure [112]. Molecular clouds have fractal geometries with a typical fractal dimension of 1.5, but it is not at all obvious what the significance of this fact is [114, 30]. A crude but useful way to characterize molecular cloud structure is to determine the fraction of cloud mass at various densities. The densities in GMCs range from a few hundred to a few million hydrogen molecules per cubic centimeter. Most (80-90%) of the material is at densities between 100-1000 cm^{-3}. About 10 % of the gas is contained in clumps and cores with mean densities of 10^4 cm^{-3} or slightly more. The distribution of dense gas through a GMC is generally not a well determined quantity. However, studies of the Orion clouds provide some indication of how such gas might be distributed [77, 122]. Dense gas is traced by molecular transitions whose excited states require high densities to be collisionally populated and which are optically thin. The most extensively used tracers for this purpose have been the the J =2-1 line of CS and the (1-1) metastable transition of NH_3, although other transitions and other lines can be equally useful.

In Figure 5 is displayed the CS(J=2-1) map of the Orion B molecular cloud [77]. Here the regions of brightest CO emission (see Figure 4) have been completely surveyed by Lada, Bally and Stark [77](hereafter LBS) for CS emission. The distribution of the CS emission and the high density gas is very clumpy. Moreover, the map appears to be dominated by a few very large clumps or cores. More than 40 dense cores were identified by LBS within the mapped region. These cores were found to have radii which ranged from 0.1 pc (the limit of telescopic resolution) to 0.5 pc. The cores were typically elongated and not circular in shape with a mean aspect ratio of 2.0 which is similar to dense cores studied in other regions [28, 15, 84]. These cores were found to range in mass between 8 - 500 $M_\odot$. The mass spectrum of these cores is displayed in Figure 6. For cores with masses in excess of 20 $M_\odot$ LBS found that the spectrum is well represented by a power-law with an index of -1.6. Since the spectral index of the cloud core mass spectrum is greater than -2, most of the dense gas in this GMC is contained in the most massive cores. Indeed, more than 50% of the dense gas detected was found to be contained within the 5 most massive cores [77]. In this regard the mass spectra of molecular cloud cores is qualitatively different that that (i.e., $\gamma_* = -2.35$) of stars which presumably form from them [69]. Since the definition of a core is arbitrary one might question the

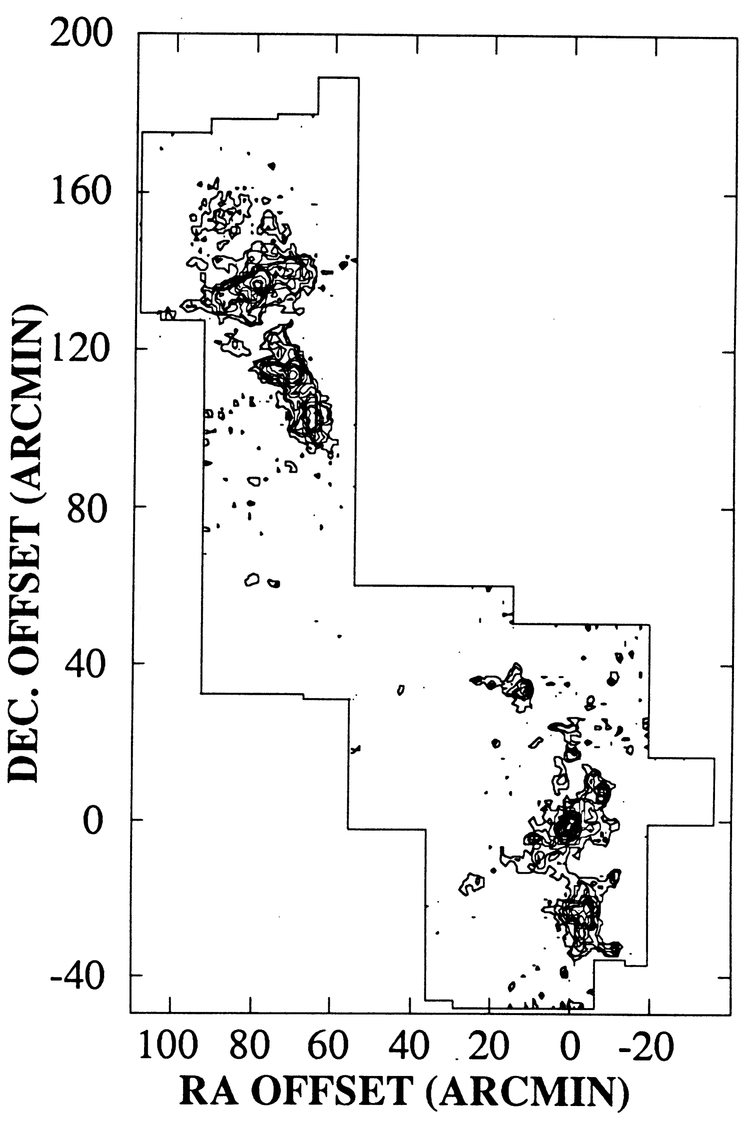

Figure 5. *Distribution of dense gas in the L1630 (Ori cloud B, see Figure 3) molecular cloud as traced by CS emission. Taken from LBS.*

significance of the derived mass spectrum. However, LBS derived the mass spectrum for the Orion B dense gas using two different clump definitions and got the same result. Moreover, it is interesting that observations of lower density clumps in 5 other GMCs as well as the Orion A cloud yield clump mass spectra with very nearly identical spectral indices despite the

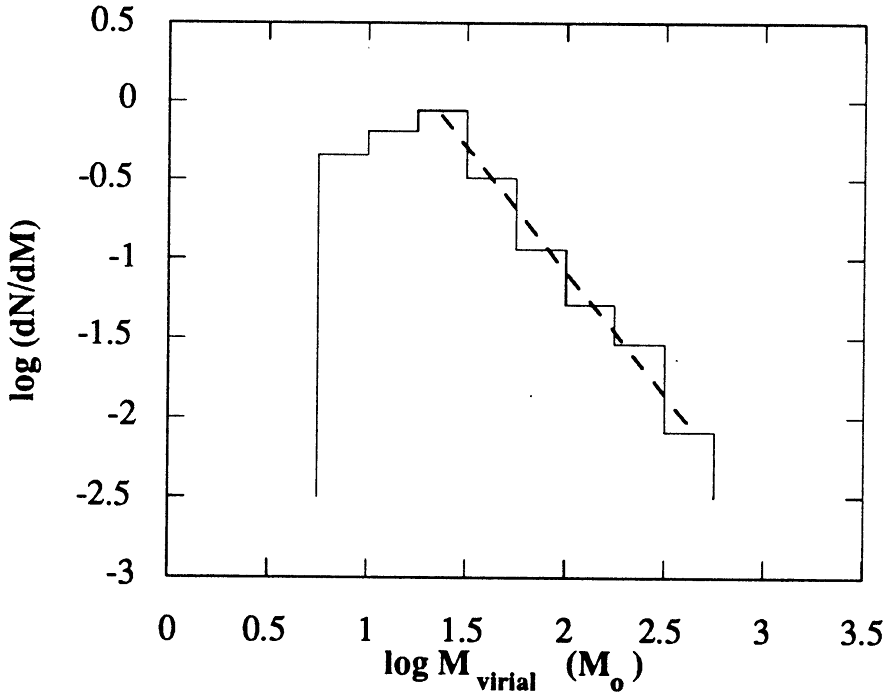

Figure 6. *The mass spectrum of dense cores in the L 1630 cloud from the study of LBS. The spectrum can be characterized by a power law with an index of -1.6.*

fact that different definitions of clumps were employed in each case [20, 122].

4. The Young Stellar Objects

4.1. CLUSTERING

Stars form in GMCs and so in this sense we expect the youngest stars to be found in groups, that is, to be spatially confined to the well defined boundaries of a GMC [68]. On the other hand, what one should expect about the spatial distribution of stars within a GMC is not at all obvious. The positions of these stars are essentially the positions of the sites of star formation activity. Knowledge of the spatial distribution of these sites and its relation to other physical properties of a star forming region (e.g., cloud structure, chemistry, temperature, and dynamical state, presence of HII regions, supernova remnants, shocks, winds, etc.) is clearly important for developing a theory of star formation. Unfortunately, stars located within a GMC are heavily extincted and difficult to observe. As a result, until recently, little was known about the distribution of young stellar objects (YSOs) within molecular clouds. The best (and only) way to get a good census of the stellar content of a GMC is through infrared observations and such observations have been only practical during the last few years. The IRAS satellite provides a data base of completely spatially sampled far-infrared observations of the sky and can be used to obtain flux limited counts of far-infrared sources in nearby clouds. However, the majority of young stars in a cloud are weak far-infrared emitters and cannot generally be detected by IRAS. Moreover, the angular resolution of IRAS was relatively coarse so that the results are often compromised by source confusion even in the nearest clouds. Near-infrared imaging surveys are much better suited to detect such stars, although such observations are themselves often limited by background source confusion.

The first cloud to be systematically surveyed at near-infrared wavelengths was the L1630 (Orion B) cloud [78, 76] which makes up the northern half of the Orion GMC complex (see Figures 3,5). A large region of the cloud surrounding the all the regions of significant CS emission was observed at 2.2 μm. Roughly half the area surveyed contained CS emission and dense gas. The observations were sensitive enough to observe a large span of the IMF and most of the stars observed had masses comparable to or less than that of the sun. The spatial distribution of these stars showed a strong tendency for the stars to be clustered. More than half ($\sim$ 58%) of all the infrared sources detected were found to be contained within three rich clusters which together subtended an angular size less than 18% of the entire area surveyed. After correcting for the presence of background/foreground star contamination, it was found that 96% of the sources *physically associated* with the cloud were contained in these 3 clusters.

Figure 7 shows the relation of the clusters to the dense gas in the cloud. The three rich clusters are spatially associated with 3 of the 5 most massive dense cores in the cloud [76]. These observations vividly demonstrate that in this cloud star formation occurs almost exclusively in: 1) rich clusters and 2) dense molecular gas. Indeed, the first phenomenon likely follows from the second. That is, if dense gas is a necessary condition for star formation then we expect most stars to form in a few rich clusters. This follows because the mass spectrum of dense gas in the cloud indicates that most of the dense gas is contained in the few most massive cores. The fact that two of the massive cores in L1630 did not produce rich clusters indicates that although dense gas may be a necessary condition for star formation it is not a sufficient condition for star formation.

Since the core mass spectra of nearby GMCs are so similar, we also ex-

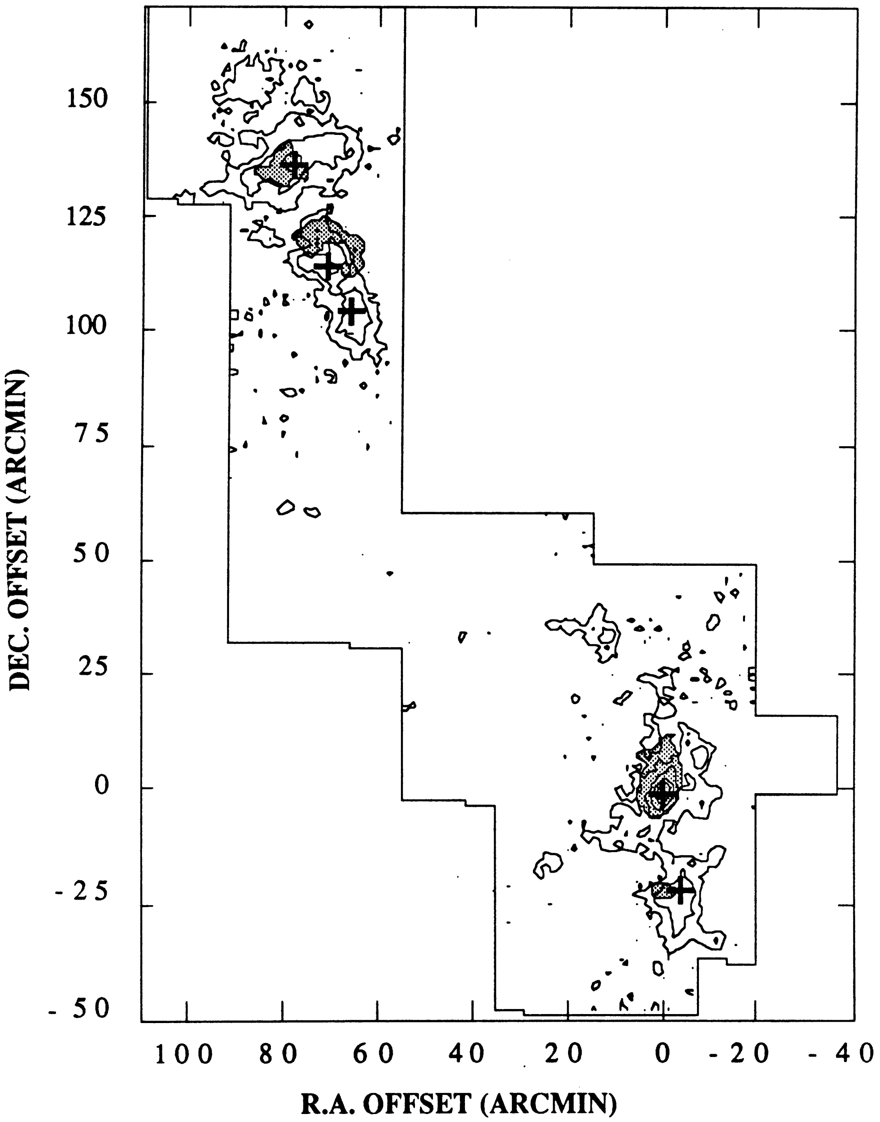

Figure 7. *The locations and extents of four embedded infrared clusters (shaded contours) compared to the distribution of dense molecular gas (solid contours) in the L 1630 cloud. Figure from Lada (1992).*

pect that these clouds should also produce most of their stars in embedded clusters as well. Indeed, infrared imaging observations have uncovered rich embedded clusters in almost every GMC studied (e.g., [105, 137]). Figure 8 shows a K-band infrared image of one such embedded cluster. However, the

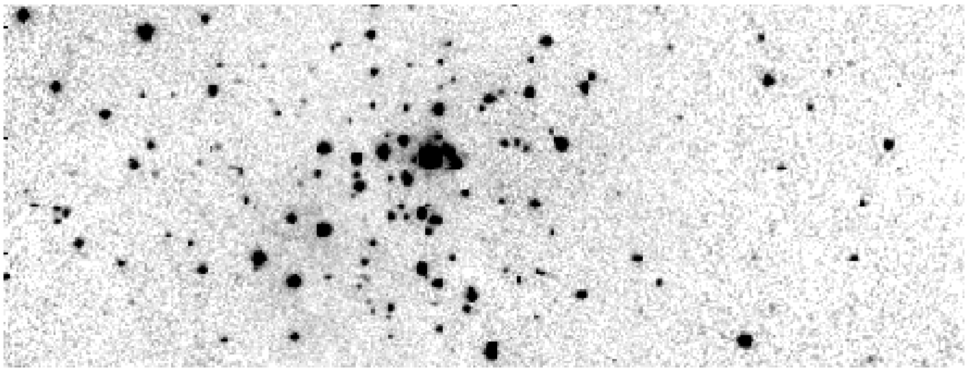

Figure 8. Example of a partially embedded infrared cluster. Deep K-band image of the young cluster NGC 2282 (Horner et al. 1996)

existing observations for most clouds are not extensive enough to determine whether clusters account for the bulk of all stars formed within them. An exceptional case is the λ Ori OB association, a fossil association which has recently emerged from and cleared away its parental GMC [31]. A systematic survey of emission line stars over the entire association shows that the majority of stars detected are also clustered [31]. The clusters are about a factor of 4 more extended than those in L1630. However, these sizes are what would be expected if the clusters started out with dimensions similar to those of L1630 (i.e., 1 pc) but became unbound after gas removal from the association (i.e., the velocity dispersion of stars in the association is measured to be ~ 2 km s^{-1}and the age of the OB cluster in its center is about 3 x 10^6 years [89, 101, 43]).

On the other hand, observations of the L1641 cloud (the Orion A cloud) present a somewhat different picture for that cloud. A spatially complete emission line survey [133] and an extensive (but not spatially complete) infrared survey [121] of the cloud suggest that in addition to stars forming in rich embedded clusters and small groups [27] there is a more distributed population of stars which could account for a significant fraction (30-40%) of all stars formed in the cloud [93, 43, 6]. The origin of this relatively large distributed population is at present unclear. However, such observations have given rise to the idea that there are two modes of star formation: a clustered mode and an isolated or distributed mode [69, 81]. In the latter circumstance, individual stars (primarily low mass stars) are formed in individual low mass cores distributed throughout a molecular cloud [68]. The prototypical example of the isolated mode of star formation is the nearby Taurus complex. With a mass of $\sim 10^4$ M$_\odot$, the Taurus dark cloud is a relatively small molecular cloud complex. The complex consists of a number of filamentary structures which contain small dense cores. These dense cores span a small range of the clump mass spectrum from about 1–40 $M_\odot$. About half of these cores contain newly formed stars [15] but typically there is only one star within an individual core. The Taurus clouds have held a very important place in star formation research. It is here that the formation of individual sun-like stars can be closely scrutinized with minimal confusion from neighboring star forming activity. Understanding the formation of individual stars is a fundamental step for the development of a comphrensive theory of star formation. However, the Taurus clouds likely do not represent the typical environment (i.e., a GMC) in which most stars form in our galaxy.

In summary it appears that most stars form in groups with a spectrum of richness ranging from relatively poor clusters with only a few stars to very rich clusters with hundreds of stars. Again, to the extent that the (stellar) mass spectra of clusters follow the mass spectra of cores from which they form, we would expect most stars in a GMC to originate in relatively rich clusters rather than in poor clusters or in isolation. We note here that most of the rich clusters that form in GMCs must be disrupted soon after they emerge from the cloud, otherwise there would be considerably more (bound) open clusters in the field than are observed [72]. This suggests that the star formation efficiency in cluster forming cores rarely reaches values as high as 50% [72, 73].

4.2. MULTIPLICITY

As is the case for field stars, there is a high frequency of multiplicity, namely binarity, among pre-main sequence stars [90]. Indeed, for stars in the Taurus T association the binary frequency is found to be higher (perhaps by a factor of 3) in the mass range surveyed than it is in the field [41, 83]. This is illustrated in Figure 9 which shows the binary frequency of pre-main sequence stars in three nearby star forming regions (Taurus, Ophiuchus and Corona Australis) compiled by Mathieu (1994). The excess of binaries at intermediate periods is due to stars in the Taurus-Auriga clouds which account for all the intermediate period binaries in Mathieu's sample. On the other hand, this excess in the pre-main sequence binary frequency is not universal. Observations of binary stars in clusters such as the rich Trapezium cluster [106] and the Pleaides [23] indicate a binary frequency distribution very similar to that of the field. Overall, studies of young stars confirm the field star results that most stars form in binary systems. Moreover, they may also suggest that most field stars were formed in environments typical of rich clusters like the Trapezium rather than in poor groups such as in Taurus (e.g., [64]). It is possible that binaries form with the same frequency

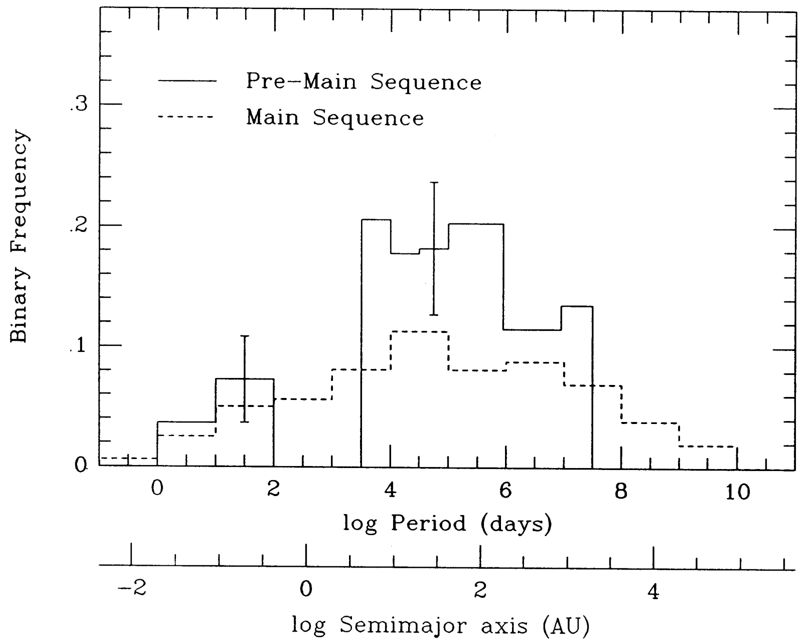

Figure 9. The binary frequency distribution for pre-main sequence stars in nearby clouds from Mathieu (1994).

both in clusters and in isolation, but in the environment of a rich cluster many binaries become disrupted very early in their evolution, while those formed in relative isolation survive for longer times.

Finally, it is important to note that binaries have been found among pre-main sequence stars of all ages, including stars near the birthline on the HR diagram. This indicates that binary systems are formed in the protostellar phase, prior to the pre-main sequence phase of evolution [90]. Indeed, this has been confirmed by the observation that a number of embedded, protostellar objects turn out to be binary systems (e.g., [134, 123]).

4.3. THE INITIAL LUMINOSITY AND MASS FUNCTIONS

The field star IMF is a globally averaged quantity, averaged over both the lifetime of the galaxy and a over a specific volume of space (i.e, the solar neighborhood). However, derivation of the IMF from observations of field stars has been hampered by two serious issues. First, observations have not been sensitive enough to adequately sample the mass function at low stellar mass, particularly near and below the hydrogen burning limit. Second, the detailed form of the IMF, particularly at masses near a solar mass and greater, is very sensitive to the uncertain history of galactic star formation [115]. Although it is often assumed that the IMF is universal in both time and space, this has never been demonstrated in any completely satisfactory way. However, in order to develop comprehensive theories for star formation and galactic evolution, it is crucial to know whether the detailed form of the IMF is universal. Are there spatial and/or temporal variations in the initial conditions and other important astrophysical parameters that can alter the process of star formation and the form of the IMF? Or is star formation such a robust process that the outcome is always an IMF of the same form?

In principle, observation of large enough groups of young or newly forming stars in different parts of the galaxy should be able to provide fundamental constraints on these questions. The smallest spatial size scale over which a meaningful determination of a luminosity function can be made is that characteristic of an open cluster. Clusters are important laboratories for studying the initial luminosity function because they consist of statistically significant groups of stars who share the common heritage of forming from the same parental cloud at the same epoch in time. Young embedded clusters are particularly useful since they are not old enough to have lost significant numbers of members due to stellar evolution or dynamical effects such as evaporation or violent relaxation [73, 72]. Thus, unlike the case for field stars, the present day stellar mass function of a young cluster is its initial mass spectrum. Moreover, low mass stars in a young cluster are brighter than at any other time prior to their evolution off the main sequence. Indeed, for very young and nearby clusters ($\leq$ a few million years) even stars with masses significantly below that of the hydrogen burning limit (i.e., brown dwarves) are readily detected at infrared wavelengths. However, study of very young clusters suffers from two disadvantages: 1) the clusters are often heavily obscured and cannot be easily observed at optical wavelengths; 2) the stars in such a cluster are mostly pre-main sequence stars and uncertain corrections for pre-main sequence evolution and non-coveality must be applied to the members to derive mass spectra from luminosity functions. Only in the last few years have advances in infrared detectors enabled the direct observation of such embedded and often obscured clusters and helped to minimize the first disadvantage. The second disadvantage requires modeling and is more difficult to overcome [137, 37, 79, 80, 100].

Two methods have been generally employed to derive the initial distribution of stellar masses from observations of young clusters. The first method involves modeling the luminosity function of an embedded cluster to derive the underlying mass function (e.g., [137, 79, 100]). The second method involves determining individual masses for the entire stellar population of a cluster by comparison of the locations of its individual member stars on the HR diagram with the predictions of PMS evolutionary models (e.g., [58, 85]). Both methods have advantages and disadvantages, but in general are complimentary.

The first method requires observation of the luminosity function of a stellar population and knowledge of its star forming history. The monchromatic luminosity function is directly obtained from photometric measurements of the members of an embedded stellar population. The measurement of a monchromatic stellar brightness is the most basic observable property of a star. With digital imaging detectors, such as CCDs and infrared array cameras, such observations generally provide the most complete set of data which can be used to investigate the form of a cluster IMF. This method for deriving the stellar mass function relies on the fact that the observed luminosity function is a product of the underlying stellar mass function and the mass-luminosity relation for the cluster stars. For a monochromatic luminosity function constructed from infrared (e.g., K band) observations:

$$dN/dm_K = dN/dlogm_* \times dlogm_*/dm_K$$

where m_k is the stellar (K) magnitude, and m_* is the stellar mass. The first term on the right hand side of the equation is the stellar mass function and the second term the mass-luminosity relation. This method is essentially that originally employed by Salpeter to derive the field star IMF. However, PMS stars, which account for most of the stars in the a young cluster, can not be characterized by a unique mass-luminosity relation. Indeed, the mass-luminosity relation for any such star is a function of time. Consequently, one must model the time-varying mass-luminosity relation for all the stars using PMS evolutionary models and knowledge of the star formation history of the cluster. The latter quantity typically can be derived by placing the stars on an HR diagram, which in turn requires multi-wavelength photometry or spectroscopy of a representative sample of the cluster members. Given PMS evolutionary models and knowledge of the star formation history of the cluster, one can then model the luminosity function to derive the mass function.

The second method requires simultaneous knowledge of both the luminosities and effective temperatures of all the stars in a cluster so that they can be individually placed on the HR diagram. This in turn requires both photometry and either colors or a spectrum of each star. For extincted clusters, spectroscopy is the preferred method of obtaining a stellar effective temperature. The advantage of this method is that the final product is the set of individual masses for all stars for which both both spectra and photometry were obtained. In other words this procedure provides a more direct and precise determination of the mass function than the first method.

Figure 10a shows the K-band luminosity function derived for the Trapezium or inner Orion Nebula cluster [137, 91]. For reference note that at the distance of Orion a one million year old star at the hydrogen burning limit would have a K magnitude of only about 12th magnitude. Also plotted are two model luminosity functions derived for the cluster using recent PMS models [29] and the mean age and age history for the cluster derived from the observations of Hillenbrand [58]. The first model is the luminosity function corresponding to Salpeter IMF, a single power-law extrapolated to below the hydrogen burning limit. Clearly, the Salpeter IMF is not consistent with the observations at low luminosities as is the case with the field stars. The underlying mass function must depart from the Salpeter form at low stellar mass. The second model luminosity function is that obtained by Meunch Lada and Lada (1999) [100] using an underlying IMF which produces the simplest best-fit to the observed luminosity function of the Trapezium cluster. This best-fit model IMF is a function consisting of three power-law segments. Below 5 $M_{\odot}$the IMF rises with decreasing stellar mass, between 0.5 and 0.1 $M_{\odot}$, the slope of the IMF is relatively flat and below 0.1 $M_{\odot}$the IMF decreases with decreasing stellar mass. (Note that at the very faint end of the luminosity function there are more stars observed than predicted by the model. This is a result of the fact that the model did not take into account contamination from reddened background stars which likely populate the lowest luminosity bins in the observed luminosity function).

The IMF derived from the modeling of luminosity function is shown in Figure 10b along with the mass function derived for the entire Orion Nebula Cluster by Hillenbrand [58]. This latter mass function was derived using optical spectra to place stars on the HR diagram and individually extract their masses. Because of sensitivity limitations, spectra were obtained for a nearly complete sample of stars with masses down to but not below the hydrogen burning limit. The two methods of deriving the IMF returned two mass functions which are in general agreement for stellar masses above the hydrogen burning limit. Moreover, the derived mass functions are, within the uncertainties, consistent with the most recent estimations of the field star IMF for masses above the hydorgen burning limit [115, 66]. Although neither the spectroscopic mass function nor the field star IMF provide much information about the form of the IMF at substellar masses, the IMF below the hydrogen burning limit is clearly constrained by the luminosity function. Current indications suggest that this brown dwarf mass function is falling with decreasing mass. The overall significance of this result is that there appears to be a peak in the initial stellar mass function at about 0.25 $M_{\odot}$.

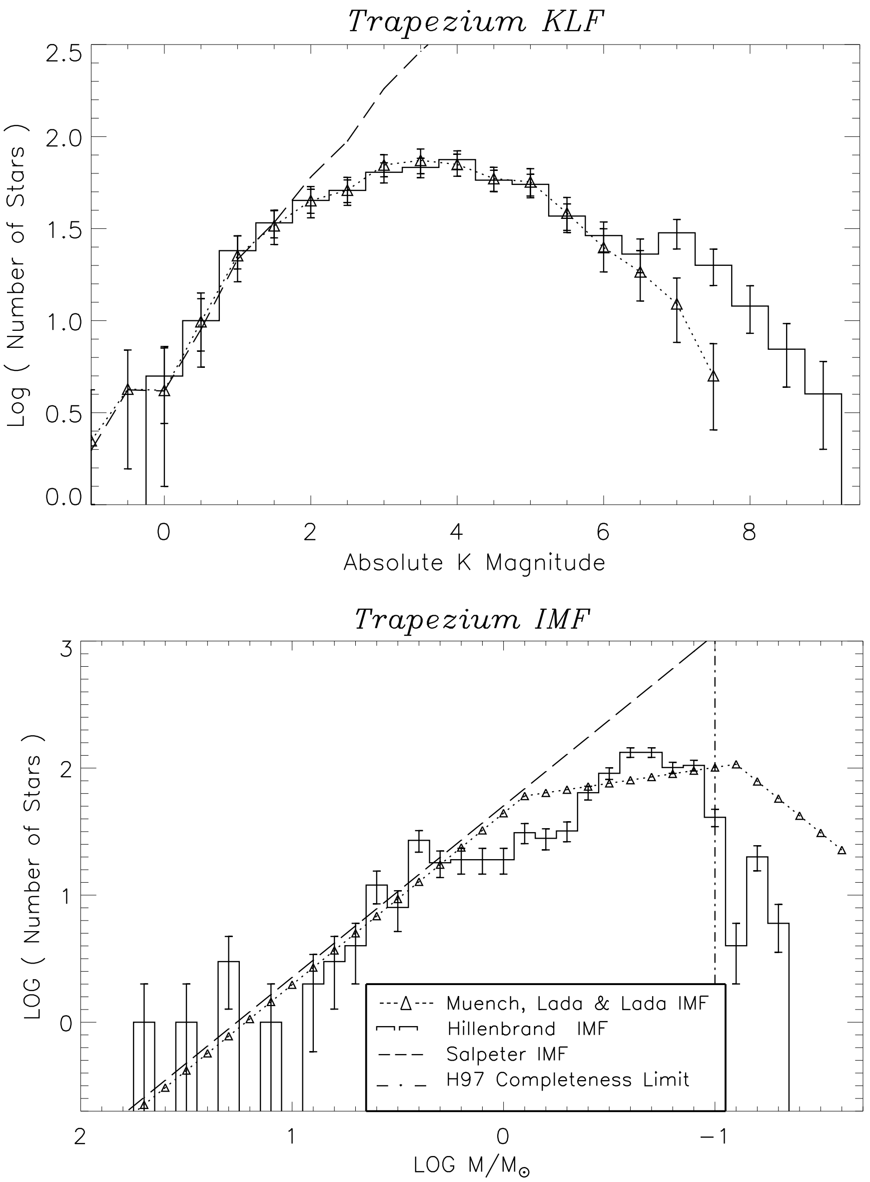

Figure 10. *a) The K band luminosity function of the Trapezium cluster in Orion. (histogram: from Zinnecker, McCaughrean and Wilking 1993 and McCaughrean et al 1996). Also plotted are two model luminosity functions. The first (dashed line) was derived assuming an underlying IMF given by the Salpeter function and is clearly a poor match to the data. The second correspnds to the three power-law mass function of Muench, Lada and Lada (1999) which was selected from a large suite of model IMFs to provide a best-fit to the observed data. b) The IMF for the larger Orion Nebula cluster derived by Hillenbrand (1997) from optical spectrosopic observations (histogram) and its completeness limit. Also plotted are the Muench et al. three power-law IMF which best fit the observations of the Trapezium luminosity function (a) and the Salpeter IMF.*

This in turn suggests that there is a characteristic mass produced by the star formation process. That that mass is close to the mass of a star at the hydrogen burning limit is very curious. Finally, it appears that the IMF for nearby young clusters is in some general sense universal and even similar to the field star IMF. This in itself suggests a robust quality to the star formation process in the galaxy, since the field star IMF is a globally averaged IMF, averaged over the age of the galaxy and a large volume of space around the sun, while the embedded cluster IMFs are instantaneous IMFs produced in very localized volumes and over relatively small spatial scales (i.e., r $\sim$ 1 pc). However, observations of older more distant open clusters suggest that important variations in the form of the IMF may be found, particularly for the more massive stars [115] and the issue of the universality of the IMF is still not satisfactorally resloved. The existing observations do suggest that significant progress on this problem can be made once complete luminosity functions are obtained for a larger sample of young embedded clusters.

4.4. SPECTRAL CLASSIFICATION: THE EVOLUTIONARY STATUS AND NATURE OF YOUNG STELLAR OBJECTS

The evolutionary status of a normal, low-mass star is essentially determined by its placement on the HR diagram which requires measurements of two quantities: luminosity and effective temperature. It is therefore no surprise that stars are most usefully classified by these two parameters (i.e., spectral type and luminosity class). The luminosity of a star is straightforwardly determined from its observed flux and its distance. The effective temperature of a star is determined from its colors or observations of temperature sensitive spectral features. This method works very well as long as a star is well behaved spectrally, that is, as long as it produces a black-body like spectrum and can be characterized by a single effective temperature. However, in this sense most young stellar objects are not normal stars. A good example is the famous young star FU Ori. The spectral type of this star is a function of the wavelength at which it is observed. Consequently, FU Ori cannot be characterized by a single effective temperature. Its placement on the HR diagram is ambiguous and the classical theory of stellar evolution cannot explain its nature.

This "abnormal" characteristic of young stellar objects is a result of their intimate physical association with the natal gas and dust from which they are formed. New stars are born within dense molecular cloud cores and throughout their formation and early evolution they are associated with varying amounts of molecular gas and dust. This circumstellar gas and dust can absorb and reprocess substantial amounts of the radiation emitted by the embedded stars significantly altering their spectral appearance. Indeed, at optical wavelengths the youngest objects are rendered completely invisible by the obscuration of opaque circumstellar dust and a significant fraction, if not all, of their luminous energy is radiated in the infrared portion of the spectrum. In general the circumstellar gas and dust associated with young stellar objects has a spatial extent considerably greater than that of a stellar photosphere. Consequently, emitting circumstellar dust, which is in radiative equilibrium with the stellar radiation field of the buried star, will exhibit a wide range of (effective) temperatures and the emission that emerges will have a spectral distribution much wider than that of a single temperature blackbody. For this reason it can be very difficult, if not impossible, to meaningfully place a YSO on an HR diagram.

Clearly, the evolutionary status of a young stellar object cannot be derived solely from knowledge of its luminosity or a single effective temperature. More complete knowledge of it spectrum, particularly at infrared wavelengths, is required. The shape of the broad–band infrared spectrum of a young stellar object depends both on the *nature* and *distribution* of the surrounding material. Clearly then, we expect that the shape of the spectrum will be a function of the state of evolution of a YSO. The earliest (protostellar) stages, during which an embryonic star is surrounded by large amounts of infalling circumstellar matter, should have a very different infrared signature than the more advanced (pre–main sequence and main sequence) stages, where most of the original star forming material has already been incorporated into the young star itself. Observations of low mass young stellar objects (mostly in isolated regions) have confirmed this expectation and such young stellar objects can be meaningfully classified by the *shapes* of their optical-infrared spectral energy distributions [68] in an empirical sequence of protostellar and early stellar evolution [3].

The spectral energy distributions of the vast majority of known (low mass) young stellar objects fall typically into one of four broad classes designated 0, I, II and III. Figure 11 illustrates spectral energy distributions (SEDs) representing each of these classes. Class 0 and I sources are characterized by SEDs which peak in the sub-millimeter and far-infrared portions of the spectrum indicating that the SEDs are dominated by emission from cold dust. These objects are the most deeply embbeded of the YSOs. They are thought to be protostellar in nature and therefore the least evolved of the YSOs. Class II and III sources are characterized by energy distributions which peak in the optical and near-infrared regions of the spectrum where emission from stellar photospheres is expected to dominate. These objects are much less reddened and correspond to the more evolved pre-main sequence and ZAMS stars.

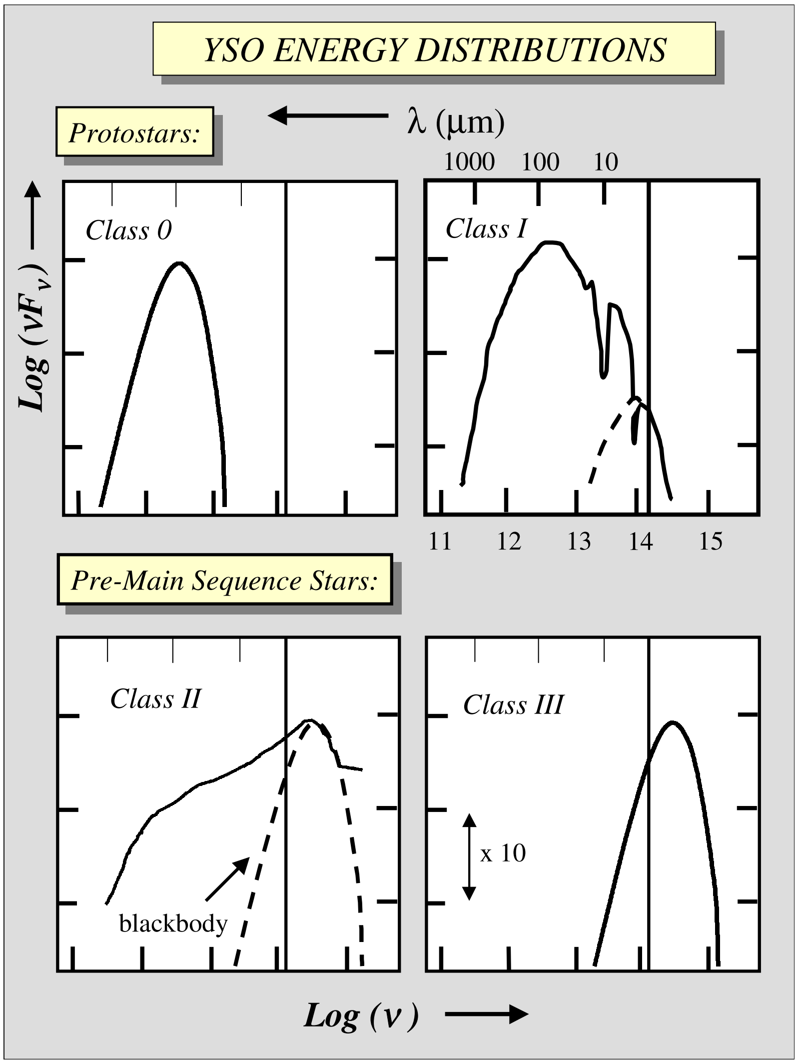

Figure 11. The empirical classification scheme for YSO spectral energy distributions. A vertical line appears at a wavelength of 2.2μm for fiducial reference in each panel. Class 0 and Class III sources have distributions whose widths are similar to single temperature blackbody functions. Class II and Class I sources display infrared excess which produces energy distributions which are broader than a single blackbody function.

However, knowledge of the source energy distribution of a YSO is, by itself, not sufficient to fully describe its the physical nature. Such objects are associated to varying degrees with a range of interesting astrophysical phenomena, such as bipolar outflows, jets, masers, HH-objects, variability, and optical/infrared emission lines. A full description or understanding of the physical natures of YSOs also requires knowledge of their relation to these various phenomena.

All things considered, YSO evolution can be divided into two primary phases. The earliest stage of evolution is the embedded phase during which protostellar evolution takes place. In this phase a star acquires the bulk of its mass through accretion of surrounding circumstellar material onto an embryonic stellar core. Throughout most of this phase the embryonic star is heavily obscured and invisible at optical wavelengths. The second phase of YSO evolution is the revealed phase, which for low mass stars corresponds to the pre-main sequence phase of early stellar evolution. By the beginning of this phase the YSO has acquired most of its final mass and has evolved to become visible at optical and near-infrared wavelengths.

4.4.1. *The Embedded Phase: Protostars*

Class I Sources. Class I SEDs are broader than a single blackbody function and peak at far-infrared or sub-millimeter wavelengths. Longward of two microns these SEDs usually rise with increasing wavelength producing a huge "excess" of infrared emission compared to that expected from a normal stellar photosphere. They typically exhibit the silicate absorption feature at 10 microns wavelength. Class I sources derive their large infrared excesses from the presence of large amounts of circumstellar dust. These sources are usually deeply embedded in dense molecular cloud cores and rarely exhibit detectable emission in the optical portion of the spectrum. However, they are detected at near-infrared (i.e., 2.2 μm) wavelengths and frequently associated with small (infrared) reflection nebulae. Indeed, a significant fraction, in some cases all, of the near-infrared emission from a Class I source is scattered light. Roughly half of the Class I sources exhibit atomic emission lines in the infrared, similar to Class II sources (e.g., [46]). Otherwise, the infrared spectra of these objects are found to be featureless and heavily veiled [46, 25, 26]. Class I sources are often associated with bipolar molecular outflows, indeed the driving sources of the vast majority of known bipolar molecular outflows are Class I objects. Class I sources are often, but not always, more luminous than Class II sources. For example, in Ophiuchus, Class I sources have luminosities in the range $\sim$ 0.2-50 $L_\odot$, with a median value of $\sim 3\ L_\odot$, while Class II sources range between 0.1 - 4 $L_\odot$with a median value of $\sim 0.6\ L_\odot$ [132, 45]. On the other hand, in Taurus, Class I sources have a median luminosity of only 0.7 $L_\odot$, the same as that of Class II sources in that cloud [60]. Class I sources are relatively rare among young stellar objects in molecular clouds and statistical arguments suggest ages of these sources of order 1-5 x 10^5 years [99, 132, 63].

Flat-Spectrum Sources. A subset of the Class I sources, these objects merit additional comment. Flat-spectrum sources have SEDs intermediate between Class I and II sources. Unlike the standard Class I source, these objects are often visible stars which display extreme T-Tauri characteristics. Indeed, the most well known member of this group is T Tauri itself. At optical wavelenghts, the spectra of these objects display little in the way of photospheric absorption features and are heavily veiled most likely by excess continuum radiation from accretion shocks at the stellar surface. Like Class I sources, these objects are also veiled at infrared wavelengths, but not as strongly. Roughly half the flat-spectrum sources display atomic and molecular absorption lines at 2.2 μm. This is significant because these are the only embedded objects for which the inner stellar component can be spectrally classified and placed on the HR diagram. These objects are found to be characterized by late-type (M) photospheres whose luminosities place them near or above the birthline ([47, 62]) similar to the youngest known Class II sources. Flat-spectrum sources appear to be objects in transition between the Class I and II phases and can be considered "optical protostars".

Class 0 Sources. These objects appear to be extreme examples of Class I objects. They are considerably more extincted and embedded than Class I sources. Their energy distributions peak at submillimeter wavelengths and most are not detected at wavelengths shortward of 20 μm. Their energy distributions have widths similar to single temperature black body functions, and unlike Class I sources they can be placed on the HR diagram. However, they are characterized by extremely low temperatures, 20-30 K! All are associated with energetic, very highly collimated bipolar molecular outflows which are typically more energetic than those associated with Class I objects [22]. On the other hand as a whole Class 0 sources are not significantly more luminous that Class I sources [22]. In addition, observations of the Ophiuchi dark cloud indicate that Class 0 sources emit significantly more submillimeter radiation than do Class I objects [7]. In particular, the circumstellar mass traced by submillimeter measurements within 1000 AU of a Class I source is usually found to amount to a fraction of a stellar mass, while for a Class 0 source this mass can be comparable to that of the central star. Based on these considerations Andre, Ward-Thompson and Barsony [9] have suggested that these sources constitute a distinct class of YSO. Whether Class 0 sources are precursors of Class I sources or represent a separate branch of early stellar evolution is not yet clear. Class 0 sources are relatively rare making up roughly 10% of embedded sources. If they are precursors of Class I sources, then their lifetimes are on the order of $\sim 10^4$

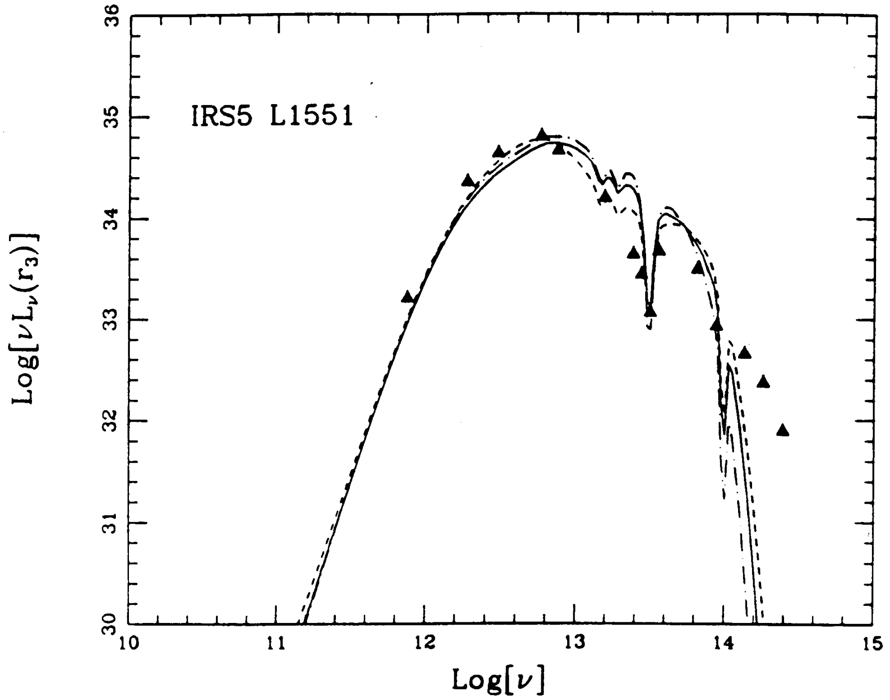

Figure 12. SED for the Class I source L 1551 IRS 5, a protostellar source in the Taurus molecular cloud. Solid and dashed lines show various rotating-collapsing isothermal protostellar models fit to the data. (From Adams, Lada and Shu 1987).

years.

On The Protostellar Nature of the Embedded Sources.

Protostars can be defined as *objects in the process of accumulating into a stellar-like configuration the bulk of the material they will ultimately contain as main sequence stars.* The identification of protostars is fundamental to the eventual development of a theory of star formation. There are four important pieces of evidence which suggest that embedded sources are indeed protostellar in nature.

First, Class I and Flat-Spectrum SEDs have been successfully modeled as systems consisting of embryonic stellar cores surrounded by circumstellar disks and massive envelopes of gas and dust whose density structure is the same as that theoretically predicted for rotating, infalling protostellar cloud cores [3, 24]. As an example, Figure 12 shows the SED of the Class I source L1551 along with protostellar models for the object. Such modelling

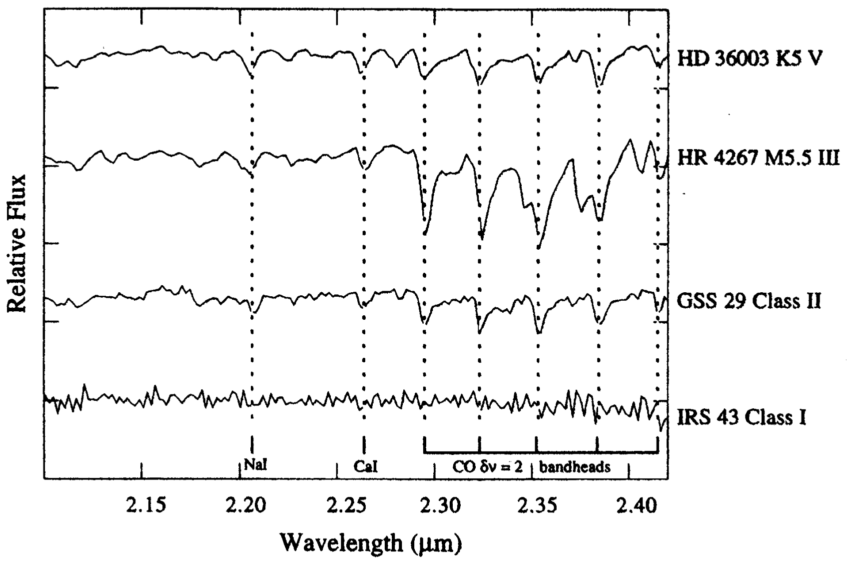

Figure 13. Infrared spectra of a low-mass Class I source, a Class II source and late type dwarf and giant spectral standard stars. (from Greene & Lada 1996).

suggests mass infall rates of $\sim 5 \times 10^{-6}\ M_{\odot}\ yr^{-1}$ for typical Class I sources. Consequently, a star can acquire a significant fraction of a solar mass over the duration ($\sim 10^5$ yrs.) of the Class I phase.

Second, as mentioned above, low resolution infrared spectroscopy has revealed that the majority of Class I sources are largely featureless as a result of the presence of strong continuum veiling [46, 25, 26]. As an example figure 13 shows the K-band, 2.2 μm spectra of a Class I source, a Class II source, a late-type field dwarf and giant, respectively. The spectrum of the Class II source exhibits absorption features which are very similar to those of the dwarf, as expected, while that of the Class I source is featureless. The lack of absorption lines in the Class I spectrum indicates the presence of an additional source of continuum flux besides that provided by the protostellar photosphere. This excess continuum flux acts to dilute or veil the absoption lines fluxes. In order to completely wash out the features at the resolution observed, the excess flux must be significantly stronger (about a factor of 5) than the continuum flux emitted by the protostellar photosphere. Moreover, this excess continuum flux must originate very close (i.e., < 0.2 AU) to the stellar surface. The most likely source of this excess continuum is either hot dust in the inner portion of an infalling protostellar envelope or emission from the inner regions of a luminous accretion disk. However, because the inner regions of a luminous accretion disk would be expected to produce its own system of detectable absorption lines (at 2μm), it is most likely that the veiling observed in Class I sources is produced by a luminous and dusty inner envelope. Dust in such an inner envelope is unlikely to be in stable orbits around the central star due to the outward pressure of radiation close to the stellar surface. However such close in material could be contained in a dynamically infalling envelope. Indeed, the same infall models which fit the SEDs of Class I sources, can produce sufficient K-band excess to completely veil protostellar infrared spectra via reprocessed light from their inner envelopes [46].

Third, essentially all Class 0 and Class I sources drive bipolar molecular outflows. The only viable source for the enormous energies which characterize the gas in molecular outflows is the release of gravitational potential energy by material falling deep into the protostellar potential well. That is, material falling directly onto the surface of an embryonic star from either an infalling circumstellar envelope or from a circumstellar accretion disk [67]. Exactly how the energy from infall and accretion is tapped to drive an energetic protostellar wind is unclear. However, the energetics of outflows are such that average protostellar mass accretion rates required to generate them must fall in the range $\dot{M}_{acc} \sim 10^{-6} - 10^{-5}$ $M_\odot$ yr^{-1} (for Class I and 0 sources, respectively [22]).

Fourth and most significant, direct kinematic evidence for infall motions appears to have been observed in a number of Class 0 sources. Under favorable circumstances, millimeter-wave molecular spectral-lines from collapsing clouds will display a kinematic signature of infall motion. This signature takes the form of an infall asymmetry in the line profile in which the red-shifted portion of an optically thick emission line is depressed relative to the corresponding blue-shifted portion. This is shown in Figure 14 In order to produce such an asymmetry, there must be an inwardly increasing excitation temperature gradient and an infall velocity whose magnitude is sufficiently large to be well resolved by the spectrometer. The first detections of this infall signature were observed toward the Class 0 sources IRAS 1629 [127] and B335 [136]. These studies further showed that the shape of the asymmetry in the line profile could be well matched by predictions using the standard infall models (e.g., [124]) to describe the velocity and density fields. Subsequent surveys of embedded sources have revealed the infall symmetry towards a substantial number ($\sim 1/3$) of Class 0 sources [48, 87]). Although few Class I sources are known to display a kinematic signature of infall, the most compelling case for infall and a protostellar status for an embedded object may be that of the Class I source HL Tau. This flat-spectrum source not only exhibits kinematic evidence for infall in millimeter-wave observations of molecular lines [52] but also in infrared observations of molecular carbon absorption-lines which originate much closer

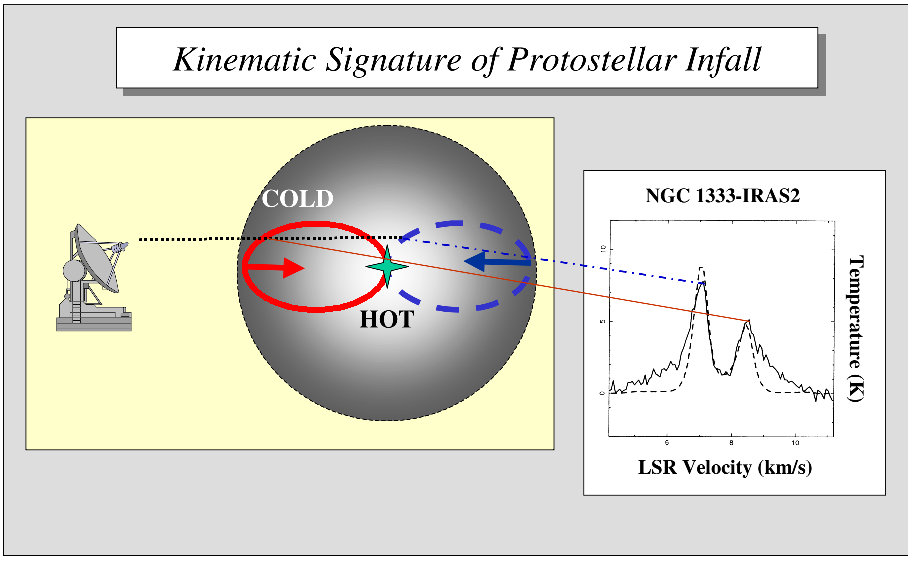

Figure 14. The kinematic signature of infall expected around a protostellar source. Oval curves represent lines of constant infall radial velocity. The dashed line represents blue-shifted gas, the solid line, red-shifted gas. Along a single line-of-sight the telescope beam intercepts the $\tau = 1$ surface in the outer, colder regions of the cloud at redshifted velocities and the inner hotter regions at blue-shifted velocites. The spectrum of NGC 1333-IRAS2 is from Ward-Thompson et al 1996.

to the stellar surface are found to be highly redshifted [44].

4.4.2. *The Revealed Phase: Pre-Main Sequence Stars*

Class II Sources. Class II SEDs peak at visible or near-infrared wavelengths. Like Class I sources the Class II SEDs are broader than a single blackbody function. Longward of two microns Class II SEDs fall with increasing wavelength usually in a power-law like fashion [75, 110, 4]. This results in an infrared excess which, though significant, is much smaller than that exhibited by Class I sources. The infrared excess indicates the presence of circumstellar material associated with the star. Figure 15 shows the composite SED of seven Class II sources. The dereddened and averaged data points are indicated by triangles and a theoretical fit to the spectrum (in which the infrared portion is modeled by a power–law function) is indicated by a solid curve.

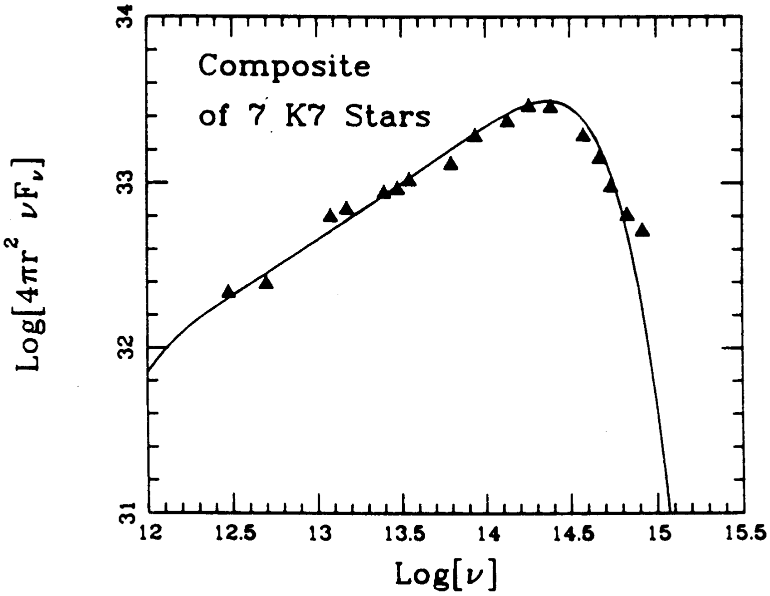

Figure 15. The composite SED of seven Class II stars along with that (solid line) of a model circumstellar disk. (From Adams, Lada and Shu 1988).

More than two decades ago Lynden-Bell and Pringle [86] predicted that T Tauri stars would display such energy distributions if they were surrounded by luminous accretion disks. Consider an optically thick and spatially thin disk that surrounds a young star and radiates everywhere like a blackbody. Imagine the disk to be composed of concentric annuli as illustrated in Figure 16 with radial dimension ΔR and area $2\pi R\Delta R$. Each annulus radiates as a blackbody of temperature $T(R)$. The emergent spectrum of the disk will then be the superposition of a series of blackbody curves of varying T(R) as shown in Figure 16. Now if $T(R) \sim R^{-n}$, the Wien laws tells us that the frequency of maximum emission scales as $\nu \sim T(R) \sim R^{-n}$. The luminosity radiated in each annulus is given by:

$$L_\nu d\nu = 2\pi R dR \sigma T(R)^4 \sim R^{2-3n} d\nu \sim \nu^{3-\frac{2}{n}}$$

Therefore, if the temperature gradient in the disk is characterized by a radial power–law, the emergent spectrum will also be characterized by a power–law slope in frequency or wavelength. For an SED, $\nu L_\nu \sim \nu^{4-\frac{2}{n}}$ or $\alpha = \frac{2}{n} - 4$ where α is the slope of the SED when plotted as a function of $\log\lambda$.

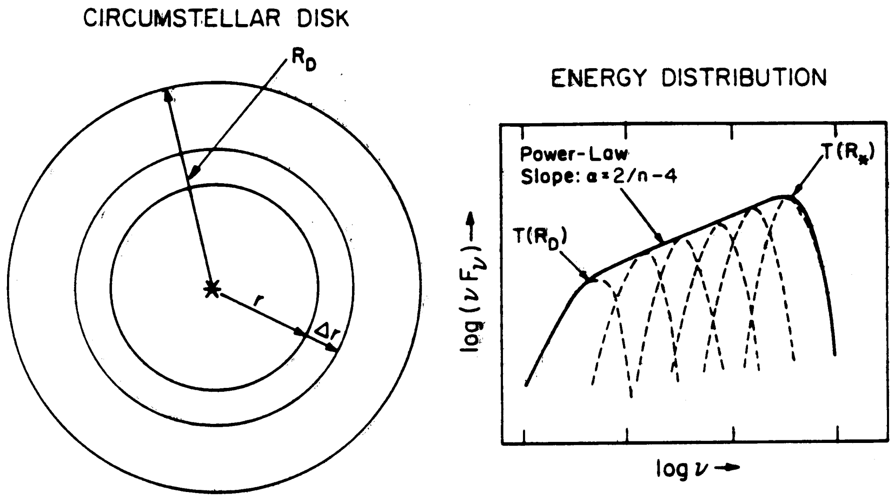

Figure 16. *Schematic diagram of a spatially thin, optically thick disk and its emergent spectral energy distribution. The disk spectrum is composed of a superposition of blackbodies of varying temperature.*

Thus the power-law shape of the infrared portion of Class II SEDs strongly suggests that the infrared excess arises in an optically thick circumstellar disk. The slope of the SED is directly related to the temperature gradient in the disk. The slopes of Class II SEDs longward of 2 microns wavelength are observed to have values in the range between -0.7 and -1.3 corresponding to a range in n, the index of the disk temperature gradient, of 0.6 to 0.75. A viscous accretion disk is predicted to produce a temperature gradient characterized by n = 0.75 [86] which corresponds to α = -1.33. This also turns out to be the same temperature gradient and spectral slope predicted for a flat purely passive disk which derives its luminosity from the reprocessing and re-radiation of light it has absorbed from the central star [2, 39]. The majority of Class II sources have shallower slopes (typically $\alpha \approx -0.7$) which suggests that they are surrounded by flared (passive) disks [61]. The excellent agreement between the predictions of disk models and observations as indicated in Figure 15 suggests that the most likely interpretation of the nature of Class II sources is that they represent young stars surrounded by circumstellar disks. They differ from Class I objects in that they lack large, massive (infalling) envelopes of gas and dust. However, it is interesting to note that the infrared to millimeter excess emission from Class II sources is sufficiently large that if the emitting material were spherically distributed and not confined to a highly flattened structure, such as a disk, the star would suffer significantly more extinction than is

Figure 17. This HST image of a resolved circumstellar disk seen in silhouette against the Orion nebula provides dramatic confirmation of the disk hypothesis for the SEDs of Class II sources. From McCaughrean and O'Dell 1996.

observed [3, 14]. Indeed, disk masses derived from detection of optically thin continuum millimeter-wave emission range between 0.01–0.1 solar masses [14].

Class II sources can be observed at optical as well as infrared wavelengths. Therefore, considerably more is known about the nature of these objects than is known about Class I or Class 0 sources. When observed optically Class II sources typically exhibit the characteristics of Classical T-Tauri stars (CTTS). Conversely, most all CTTS stars possess Class II SEDs. Classical T-Tauri stars are low mass, pre-main sequence, emission-line variable stars. In addition to excess infrared continuum emission, these stars also exhibit excess emission at ultraviolet wavelengths. The optical spectra of CTTS contain Hydrogen emission lines and frequently various forbidden emission lines as well. The forbidden lines are believed to arise in stellar winds originating near the surface of the star. Typically these lines are observed to be blue-shifted and the absence of red-shifted emission is interpreted as strong supporting evidence for the presence of an occulting disk close to the stellar surface [33, 10]. The origin of the Balmer emission lines is more mysterious. Analysis of these lines provides evidence for both mass loss and mass accretion in these objects [16]. However, both the mass accretion and ultraviolet excess are believed to be consequences of disk accretion onto the stars [16]. The accretion rates are typically $\sim 10^{-8}$ $M_\odot$

yr^{-1} (e.g., [49]) and though significant, are relatively low compared to the typical infall rates encountered in protostellar evolution. Because they are visible, CTTS can be placed on the HR diagram, and when their positions are compared to theoretical PMS tracks one derives ages for CTTS usually between 10^6 and 4 x 10^6 years. However, because the theoretical tracks are calculated assuming diskless PMS stars, it is not clear how they actually relate to the positions of accreting CTTS on the HR diagram. Class II sources are relatively common in star formation regions where they typically outnumber Class I sources by more than 10-to-1.

In summary, Class II sources have been observed over three decades in frequency and over this entire range their SEDs are well matched by the predictions of model stars with circumstellar disks. UV observations and optical spectral-line observations provide additional supporting evidence for the presence of such circumstellar disks and further indicate that these stars are actively accreting material from their disks.

Class III Sources. Class III SEDs typically peak at visible and infrared wavelengths for low mass stars and decrease longward of two microns more steeply than Class II sources. Since their shapes are more or less similar to single temperature blackbodies, the energy distributions of Class III sources are easily interpreted as arising from extincted or unextincted photospheres of young stars. By definition these stars display no infrared excess. However, their light still could be substantially extinguished by foreground dust.

Extinction attenuates the spectrum of a YSO by a factor of $\exp(-\tau_\nu)$ and since $\tau_\nu \sim \nu$, for interstellar dust, then $F_\nu \sim \exp(-\nu)$ and it is difficult to distinguish such a spectrum from the high frequency side of a blackbody function where $F_\nu \sim \exp(-\frac{h}{kT}\nu)$. Thus an extincted star has an energy distribution similar to a blackbody but with the high frequency end exponentially extinguished and the peak displaced toward lower frequencies thus giving the appearance of being "reddened".

Class III sources are basically free of any significant amounts of circumstellar gas and dust and can be readily placed on the HR diagram. Class III sources are found to lie above the main sequence and can be thought of as "classical" pre-main sequence stars in the sense that their positions on the HR diagram can be unambigously compared to predictions of theoretical PMS tracks [129]. Comparison with such theoretical tracks shows that the ages of Class III sources range from roughly 10^6 years to more than 10^7 years. Although most Class III sources have ages > 5 x 10^6 years, and are likely candidates for post-T Tauri stars (PTTS), a significant number have ages which overlap with those of Classical T Tauri Stars (CTTS) [129]. Since they lack infrared and ultraviolet excesses and are not strong emission-line emitters, these stars are difficult to distinguish from foreground and background stars in star formation regions. Thus it is difficult to obtain a census of their relative numbers. However, compared to field stars, Class III sources are relatively strong (but variable) X-Ray sources and can be identified in X-Ray surveys. In the Taurus region such observations suggest that the population of Class III sources is at least comparable in size to that of Class II sources. Older Class III objects are also found to extend well beyond the boundaries of star formation regions in X-ray surveys [102]. Class III sources typically produce little or no Hα line emission. All Class III sources are therefore Weak-lined T Tauri stars (WTTS). (Optical astronomers classify PMS stars with Hα equivalent widths less than 10 Angstroms as WTTS and PMS stars with Hα equivalent widths greater than 10 Angstroms as CTTS.)

5. The YSO Evolutionary Sequence

Although the SED classes (0, I, II, III) discussed above correspond to distinct physical classes of YSOs, the variation in the shapes of the energy distributions from Class 0 to III is quasi continuous and for some purposes can be usefully parameterized by an SED spectral index [68] or a "bolometric" temperature [98]. This variation in SED shape represents an evolutionary sequence corresponding to the gradual dissipation of gas and dust envelopes around newly formed stars [68]. Adams, Lada and Shu [3] were able to theoretically model this empirical sequence as a more or less continuous sequence of early stellar evolution from protostar to young main sequence star using the self-consistent physical theory of rotating collapsing isothermal spheres as the initial condition (see also [117, 54]). In the current version of this theoretical picture Class 0 and Class I sources are the youngest and least evolved objects, indeed, true protostars, objects assembling the bulk of the mass they will ultimately contain when they arrive on the main sequence. They consist of a central embryonic (hydrostatic) stellar core surrounded by a circumstellar disk and are steadily gaining mass from infall and accretion of surrounding matter. Class III sources are the most evolved objects. For these objects the vast majority of the original star forming material has been either all incorporated into the star or removed from its vicinity. The vast majority of low mass stars probably pass through these stages during their formation. However, the fact that some Class III sources have similar ages as Class II sources, suggests that the duration of the various phases may be different for different stars, even those of similar mass.

5.1. THE PIVOTAL ROLE OF BIPOLAR OUTFLOWS

To evolve from Class 0 to I to II requires the removal or dissipation of the circumstellar material in the protostellar infalling envelope. To evolve

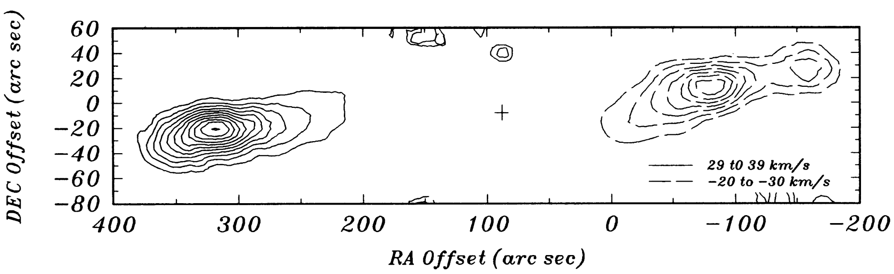

Figure 18. *An example of a bipolar molecular outflow. Shown here are the high velocity lobes of the NGC 2264G outflow traced by emission in the J=2→1 transition of CO. A cross marks the location of a deeply embedded Class 0 protostellar object. From Lada and Fich (1996).*

from Class II to Class III requires clearing of the circumstellar disk. In principle, the clearing of circumstellar gas and dust could be accomplished by accreting all the surrounding material onto the star itself. This might occur in massive cloud cores which form clusters via fragmentation. There is some recent evidence to suggest that such fragmentation may produce clumps with a mass spectrum similar to the stellar IMF [95, 125]). In which case a star could evolve from the Class I to III phase once it simply accreted the entire mass of the fragment form which it was born. On the other hand, this possibility conflicts with the observation that star formation occurs with considerable inefficiency: the cores from which stars form contain much more mass than the stars themselves, and most of the surrounding material cannot end up inside the star. This suggests that at some point very early on in the evolution of a young stellar object the cloudy material from which it grows must be physically removed by some active agent.

This agent is most likely the energetic bipolar outflow which is ignited early in the protostellar stage of evolution [119, 12, 67, 13, 40, 11]. Bipolar outflows and associated jets, masers and Herbig-Haro objects, are generated almost exclusively by embedded objects (Class 0 and I). They are very rarely associated with Class II or III stars. Bipolar molecular outflows are individually energetic enough to disrupt cloud cores and collectively even powerful enough to have a significant impact on the dynamics and structure of an entire GMC [88]. In fact, the molecular outflows generated by a population of embedded YSOs may be able to generate the turbulent pressure that keeps GMCs from global collapse, thereby solving one of the outstanding problems of cloud dynamics.

Essentially all Class I and Class 0 sources drive molecular outflows, yet these objects are supposed to be protostellar in nature, their dynamics dominated by infall and accretion. This presents a paradox: how is a star

Figure 19. *An example of a bipolar outflow visible at optical wavelengths. This is an HST image of the Herbig-Haro objects HH 1 and HH 2. The visible emission originates in shocks resulting from the impact of high velocity jets on ambient cloud material. A deeply buried Class I source, located in the dark cloud core between the two lobes, drives this well known outflow.*

simultaneously a source of both outflow and infall, how does a star grow by losing mass? The resolution of this paradox, as mentioned earlier, must be that outflows are driven by infall and accretion.

Magnetic fields and angular momentum may play critical roles in enabling the transfer of energy from infalling to outflowing gas. To visualize how this might work, consider a rotating infalling protostellar envelope. Because of the conservation of angular momentum the trajectories of infalling material become curved as they near the growing stellar object at the center of the potential well. As a result, most of the infalling gas misses the star and falls into the equatorial plane forming an extended disk. Consequently for a rotating protostar most of the mass that ends up on the star must be accreted from the surrounding disk. In order for material to flow through the disk and onto the protostar, the material must lose both energy and angular momentum. If the mass of the disk is not much larger than that of the central object, the material in the disk should rotate differentially in Keplerian fashion. Gas falling through such a disk will reach the surface of the central star with an orbital velocity and specific angular momentum which is relatively high compared to that in the star. If this material is added to the star it will spin up the star. The star will quickly reach break up equatorial velocities at which point material can no longer be added to it. A centifugal barrier prevents the further growth of the protostar. Thus the process of star formation can only proceed if the incoming gas somehow can lose additional angular momentum in the process of accreting onto the star or if the star can somehow spin down while accretion is taking place.

Angular momentum can be carried away from a star by a stellar wind. *Consequently, a protostar may be able to gain mass only if it simultaneously* *loses mass*. To allow star formation to continue the rate of mass loss from the wind should be a fraction of the mass accretion rate i.e.,

$$\dot{M}_{wind} = f\dot{M}_{accretion}$$

where the fraction f is determined by the physics of the wind generating mechanism. The ideal protostellar wind is one that carries away little mass but lots of angular momentum. A number of recent investigations have shown that centrifugally–driven hydromagnetic winds are potentially capable of doing the job [107]. Such winds could be driven from either magnetized circumstellar disks [107] or from the surfaces of central protostars [118]. Thus the natural consequence of star formation in rotating, magnetic cloud cores may be the formation of protostar-disk systems which generate powerful outflows and in doing so resolve the paradox of the protostar which gains mass by losing mass. An additional consequence of such "accretion driven" outflow is that as a protostar evolves, its outflow disrupts the surrounding core ultimately limiting the mass which can fall onto the central star. As the protostellar envelope disperses, the reservoir of infalling material available to drive disk accretion and mass outflow also diminishes and the YSO evolves to progressively less active states (i.e., Class I-II-III), consistent with observations and the evolutionary spectral sequence described earlier.

5.2. EPISODIC ACCRETION?

Finally, it is presently uncertain whether the infall/accretion/outflow process is steady over time. The observation that outflows from Class 0 sources are more energetic than those from Class I sources suggests that the infall/accretion declines from the Class 0 to Class I phases [22]. Clearly there is a dramatic decrease in outflow activity by the Class II and III stages suggesting an equally drastic drop in the rate of infall/accretion. Moreover, there is a growing body of evidence indicating that episodic mass ejection may be an important aspect of the protostellar evolution of low mass stars [57, 108, 50]. There is a subset of YSOs (*FU Ori objects*), originally identified by Herbig, [57] which are known to undergo intense outbursts of light. These outbursts, which can increase the luminosity of the star by a factor as much as 100 in a few years, are most likely due to dramatic, apparently episodic, increases in disk accretion onto the star [50]. Although most often identified by specific optical spectral characteristics [50], these objects typically turn out to be Class I sources. It is possible that FU Ori outbursts occur throughout protostellar evolution. Although infall rates for protostars are high, the relatively low luminosities (~ 1 $L_{\odot}$) of some Class I sources suggest they are simultaneously characterized by significantly lower disk accretion rates [60]. The infall/accretion luminosity for a protostar is given by:

$$L_{accretion} = \frac{1}{2} \times \frac{GM_*\dot{M}}{R_*}$$

For nominal Class I parameters this can be expressed as:

$$L_{accretion} = 5.5 \times [\frac{M_*(M_\odot)}{0.25}][\frac{\dot{M}(M_\odot \mathrm{yr}^{-1})}{2 \times 10^{-6}}][\frac{10^{11}}{R_*(\mathrm{cm})}] \ \ L_\odot$$

This is the luminosity due to infall and accretion assuming all the infalling material reaches the surface of the star. If most of the infalling material lands on the disk and does not accrete through it at the same rate as the infall onto it (i.e., $\dot{M}_{acc} < \dot{M}_{infall}$), then $L_{accretion}$ would be smaller than the steady state value. However, in this situation the disk would grow in mass. This could not continue indefintely and eventually the disk would have to dump significant amounts of mass onto the surface of the central protostar. Such a discharge would presumably result in an FU Ori outburst. The resulting accretion rate would be expected to be somewhere in the range 10^{-4} $M_\odot$ yr^{-1} and 10^{-5} $M_\odot$ yr^{-1} (corresponding respectively to the inferred accretion rates of FU Ori and L1551, two representative FU Ori objects). Depending on which rate is typical, we would expect anywhere from 5% to 50% of Class I sources to be in outbust at any one epoch of history (since the lifetime of a Class I source is roughly 10^5 yrs and the final mass of its central star is roughly 0.5 $M_\odot$). Spectroscopic surveys of the Ophiuchus and Taurus clouds [46] suggest that approximately 3% of the Class I sources in those clouds display the spectroscopic signature of an FU Ori star. Perhaps this favors luminous, short lived outbursts throughout the late protostellar phase. On the other hand, many protostellar sources appear to be reasonably luminous and do not display the spectroscopic signature of an FU Ori object. These sources may be actively accreting at the steady-state rate. Clearly more observations of embedded objects are required to determine how significant FU Ori type outbursts are for protostellar evolution.

6. Concluding Remarks

Over the last few years a coherent picture of protostellar and early stellar evolution (for at least isolated, low mass objects) has been derived from observations and buttressed by theory. Still, much remains to be done in order to achieve the important goal of a complete and predictive theory of star formation. In particular, our understanding of the origin of high mass stars, the origin of the IMF, the nature of bipolar outflows and the process of star formation in embedded clusters is still far from complete. These are among the many interesting problems that remain at the frontier of star formation research as we begin the twenty-first century.

References

1. Abt, H.A. & Levy, S. 1976 *Astrophys. J. Suppl. Ser.*, **30** 273.
2. Adams, F.C., & Shu, F. 1986 *Astrophys. J.*, **308** 836.
3. Adams, F.C., Lada, C.J., & Shu, F. 1987 *Astrophys. J.*, **312** 788.
4. Adams, F.C., Lada, C.J., & Shu, F. 1988 *Astrophys. J.*, **326** 825.
5. Allen, C.W. 1973 *Astrophysical Quantities*, (Athlone Press: London).
6. Allen, L. & Hillenbrand, L. 1998 in *The Orion Complex Revisited*, eds. M.J. McCaughrean and A. Burkert (ASP Conference Series), in press.
7. Andre, P. & Montmerle, T. 1994 *Astrophys. J.*, **420** 837.
8. Andre, P. 1994 in *The Cold Universe*, eds. T. Montemerle, C.J. Lada, F. Mirabel and J. Tran Thanh Van, (Paris, 1994) 179.
9. Andre, P., Ward-Thompson, D. & Barsony, M. 1993 *Astrophys. J.*, **406** 122.
10. Appenzeller, I., Jankovics, I & Ostreicker, R. 1984 *Astron. Astrophys.*, **141** 108.
11. Bachiller, R. 1996 *Ann. Rev. Astron. Astrophys.*, **34** 111.
12. Bally, J. & Lada, C.J. 1983 *Astrophys. J.*, **265** 824.
13. Bally, J. & Lane, A.P. 1991 in *The Physics of Star Formation and Early Stellar Evolution*, eds. C.J. Lada and N.D. Kylafis, (Kluwer Academic Publishers: Dordrecht), p. 471.
14. Beckwith, S.V.W., Sargent, A.I., Chini, R. & Gusten, R. 1990 *Astron. J.*, **99** 924.
15. Benson, P. & Myers, P. 1989 *Astrophys. J. Suppl. Ser.*, **71** 89.
16. Bertout, C. & Basri, G. 1991 in *The Physics of Star Formation and Early Stellar Evolution*, eds. C.J. Lada and N.D. Kylafis, (Kluwer Academic Publishers: Dordrecht), p. 649.
17. Blaauw, A. 1964 *A.R.A.A.* **2** 213.
18. Blaauw, A. 1991 in *The Physics of Star Formation and Early Stellar Evolution*, eds. C.J. Lada and N.D. Kylafis, (Kluwer Academic Publishers: Dordrecht), p. 125.
19. Blitz, L. 1980 in *Giant Molecular Clouds in the Galaxy*, eds. P Solomon and M. Edmunds, (Pergamon, Oxford) p. 1.
20. Blitz, L. 1991 in *The Physics of Star Formation and Early Stellar Evolution*, eds. C.J. Lada and N.D. Kylafis, (Kluwer Academic Publishers: Dordrecht), p. 3.
21. Bok, B.J. 1934 *Harvard Circ. No. 384.*
22. Bontemps, S., Andre, P., Tereby, S. and Cabrit, S. 1996 *Astron. Astrophys.*, **311**, 858.
23. Bouvier, J., Rigaut, F. & Nadeau, D. 1997 *Astron. Astrophys.*, **326**, 1023.
24. Calvet, N., Hartmann, L., Kenyon, S. & Whitney, B. 1994 *Astrophys. J.*, **434** 330.
25. Casali, M.M. & Erioa, C. 1996 *Astron. Astrophys.*, **306**, 427.
26. Casali, M.M, & Matthews, H.F. 1992 *Monthly Notices Roy. Astron. Soc.*, **258**, 399.
27. Chen, H., Tokunaga, A., Strom, K. & Hodapp K. 1993 *Astrophys. J.*, **407** 639.
28. Clemens, D. & Barvanis, R. 1988 *Astrophys. J. Suppl. Ser.*, **68** 257.
29. D'Antona, F. & Mazzitelli, I. 1994 *Astrophys. J. Suppl. Ser.*, **41** 467.
30. Dickman, R.L., Horvath, M.A., & Margulis, M. 1990 *Astrophys. J.*, **365** 586.
31. Duerr, R., Imhoff, K. & Lada, C.J. 1982 *Astrophys. J.*, **261** 135.
32. Duquennoy, A. & Mayor, M. 1991 *Astron. Astrophys.*, **248**, 485.
33. Edwards, S. *et al.*, 1987 *Astrophys. J.*, **321** 473.
34. Elmegreen, B.G. & Lada, C.J. 1976 *Astron. J.*, **81** 1089.
35. Elmegreen, B.G. & Lada, C.J. 1977 *Astrophys. J.*, **214**, 725.
36. Evans, N.J. *et al.* 1994 *Astrophys. J.*, **424** 793.
37. Fletcher, A. & Stahler, S. 1994 *Astrophys. J.*, **435** 313.
38. Fischer, D. & Marcy, G. 1992 *Astrophys. J.*, **396**, 178.
39. Friedjung, M. 1985 *Astron. Astrophys.*, **146** 336.

40. Fukui., F. *et al.*, 1993 in *Protostars and Planets III*, eds. E. H. Levy and J. I. Lunine, (Arizona: Tucson), p. 603
41. Gehz, A. 1993 Unpublished PhD Dissertation, Caltech.
42. Goldreich, P. and Kwan, J. 1974 *Astrophys. J.*, **89** 441.
43. Gomez, M. & Lada, C.J. 1998 *Astron. J.*, **115** 1524.
44. Grasdalen, G., Sloan, G., Stout, N., Strom, S. & Welty, A. 1989 *Astrophys. J.*, **339** 37.
45. Greene, T.P. *et al.* 1994 *Astrophys. J.*, **434** 614.
46. Greene, T.P. & Lada, C.J. 1996 *Astron. J.*, **112** 2184.
47. Greene, T.P. & Lada, C.J. 1997 *Astron. J.*, **114** 2157.
48. Gregersen, E.M., Evans, N.J., Zhou, S., & Choi, M. 1997. *Astrophys. J.*, **484**, 256.
49. Gullbring, E., Hartmann, L., Berinco, C. & Calvet, N. 1998 *Astrophys. J.*, **492** 323.
50. Hartmann, L. & Kenyon S. J. 1996 *Ann. Rev. Astron. Astrophys.*, **34**, 207.
51. Hayashi, C. 1966 *Ann. Rev. Astron. Astrophys.*, **4** 171.
52. Hayashi, M., Ohashi, N. & Miyama, S.M., 1993 *Astrophys. J. Letters*, **418** 71.
53. Heiles, C., Goodman, A.A., & Zweibel, E. 1993 in *Protostars and Planets III*, eds. G. Levy and J. Lunine, (University of Arizona Press, Tucson) p. 279.
54. Henriksen, R., Andre, P. & Bontemps, S. 1997 *Astron. Astrophys.*, **323**, 565.
55. Henyey, L.G., LeLevier, R. & Levee, R.D. 1955 *Publ. Astron. Soc. Pacific*, **67** 154.
56. Herbig, G. 1962 *Adv.Astr.Ap* **1** 47.
57. Herbig, G. 1977 *Astrophys. J.*, **217** 693.
58. Hillenbrand, L. 1997 *Astron. J.*, **113**, 1733.
59. Horner, D.L., Lada, E.A., & Lada, C.J. 1997 *Astron. J.*, **113** 1788.
60. Kenyon, S.J. & Hartmann, L. 1995 *Astrophys. J. Suppl. Ser.*, **101**, 117.
61. Kenyon, S.J. & Hartmann, L. 1987 *Astrophys. J.*, **323** 714.
62. Kenyon, S.J., Brown, D.L., Tout, C.A., & Berlind, P. 1998, *Astron. J.*, **115** 2491.
63. Kenyon, S.J., Hartmann, L., Strom, S.E., Strom, K.M. 1990 *Astron. J.*, **99** (1990) 869.
64. Kroupa, P. 1995 *Monthly Notices Roy. Astron. Soc.*, **277** 1491.
65. Kroupa, P., Tout, C. & Gilmore, G. 1990 *Monthly Notices Roy. Astron. Soc.*, **244** 76.
66. Kroupa, P., Tout C. & Gilmore, G. 1993 *Monthly Notices Roy. Astron. Soc.*, **262** 545.
67. Lada, C.J. *Ann. Rev. Astron. Astrophys.*, **23** 267.
68. Lada, C.J. 1987 in *I.A.U. Symposium No. 115: Star Forming Regions*, eds. M. Peimbert and J. Jugaku, (Dordrecht, Reidel), p. 1.
69. Lada, C.J. 1991 in *The Physics of Star Formation and Early Stellar Evolution*, eds. C.J. Lada and N.D. Kylafis, (Kluwer Academic Publishers: Dordrecht), p. 329.
70. Lada, C.J. & Fich M. 1996 *Astrophys. J.*, **459** 638.
71. Lada, C.J. & Kylafis, N.D. 1991 *The Physics of Star of Star Formation and Early Stellar Evolution*, (Dordrecht: Kluwer).
72. Lada C.J. & Lada, E.A. 1991 in *The Formation and Evolution of Star Clusters*, ed. K. Janes (ASP, San Francisco,) p. 3.
73. Lada, C.J., Margulis, M. & Dearborn, D. 1984 *Astrophys. J.*, **285** 141.
74. Lada, C.J., Young, E.T., & Greene, T. 1993 *Astrophys. J.*, **408** 471.
75. Lada, C.J. & Wilking, B.A. 1984 *Astrophys. J.*, **287** 610.
76. Lada, E.A. 1992 *Astrophys. J. Letters*, **393** 25.
77. Lada, E.A., Bally, J. & Stark, A. 1991 *Astrophys. J.*, **368** 432.
78. Lada, E.A., DePoy, D.L., Evans, N.J. & Gatley, I. 1991 *Astrophys. J.*, **371** 171.
79. Lada, E.A. & Lada, C.J. 1995 *Astron. J.*, **109** 1682.
80. Lada, E.A., Lada, C.J. & Muench, G. 1998 in *The Stellar Initial Mass Function*, ASP Conference Series vol 142 eds. G Gilmore and D. Howell (ASP: San Francisco) 107.
81. Lada, E.A., Strom, K.M., & Myers, P.C. 1993 in *Protostars and Planets III*, eds.

G. Levy and J. Lunine, (University of Arizona Press, Tucson) p. 245.
82. Larson, R.B. 1981 *Monthly Notices Roy. Astron. Soc.*, **194** 271.
83. Leinert, Ch. 1993 *et al. Astron. Astrophys.*, **278**, 129.
84. Loren, R. 1989 *Astrophys. J.*, **338** 902.
85. Luhman, K.H., Rieke, G.H., Lada, C.J. & Lada, E.A. 1998 *Astrophys. J.*, **508** 347.
86. Lynden-Bell D. & Pringle, J. 1974 *Monthly Notices Roy. Astron. Soc.*, **168** 168.
87. Mardones, D. *et al.* 1997 *Astrophys. J.*, **489** 719.
88. Margulis, M., Lada, C.J. & Snell, R.N. 1989 *Astrophys. J.*, **333** 316.
89. Mathieu, R.D. 1987 in *I.A.U. Symposium No. 115: Star Forming Regions*, eds. M. Peimbert and J. Jugaku, (Dordrecht, Reidel), p. 61.
90. Mathieu, R.D. 1994 *Ann. Rev. Astron. Astrophys.*, **32** 465.
91. McCaughrean, M. J., Zinnecker, H., Rayner, J. Stauffer, J. 1995 in *Proceedings of the ESO Workshop: The Bottom of the Main Sequence and Beyond*, (ed. C.G. Tinney), (Heidelberg: Springer) 207.
92. McCaughrean, M.J., & O'Dell, C.R. 1996 *Astron. J.*, **111** 1979.
93. Meyer, M.R. and Lada, E.A. 1998 in *The Orion Complex Revisited*, eds. M.J. McCaughrean and A. Burkert (ASP Conference Series), in press.
94. Mihalas, D. and Binney, J. 1981 *Galactic Astronomy*, (Freeman: San Francisco), p 217.
95. Motte, F., Andre, P. & Neri, R. 1998 *Astron. Astrophys.*, **336**, 150.
96. Mouschovias, T. 1976 *Astrophys. J.*, **207** 141.
97. Mouschovias, T. 1991 in *The Physics of Star Formation and Early Stellar Evolution*, eds. C.J. Lada and N.D. Kylafis, (Kluwer Academic Publishers: Dordrecht), p. 61.
98. Myers, P.C. & Ladd E. F. 1993 *Astrophys. J. Letters*, **413** 47.
99. Myers, P.C. *et al.*, 1987 *Astrophys. J.*, **319** 340.
100. Muench, G., Lada, E.A. & Lada, C.J. 1998 *Astrophys. J.*, in preparation.
101. Murden. P.G., & Penston, M.V. 1977 *Monthly Notices Roy. Astron. Soc.*, **181** 657.
102. Neuhauser, R. 1997 Science, **276** 1363.
103. Palla F. & Stahler, S.W. 1993 *Astrophys. J.*, **418** 414.
104. Parker, N.D., Padman, R., Scott, P. & Hills, R. 1991 *Monthly Notices Roy. Astron. Soc.*, **234** 442.
105. Phelps, R.L. & Lada, E.A. 1997 *Astrophys. J.*, **477** 176.
106. Prosser, C. *et al. Astrophys. J.*, **421** 517.
107. Pudritz, R., Pelletier, G., Gomez de Castro, A.I. 1991 in *The Physics of Star Formation and Early Stellar Evolution*, eds. C.J. Lada and N.D. Kylafis, (Kluwer Academic Publishers: Dordrecht), p. 539.
108. Reipurth, B. 1989 *Nature* **340** 42.
109. Roberts, M.S. 1957 *P.A.S.P.* **69** 59.
110. Rucinski, S.M. 1985 *Astron. J.*, **90** 2321.
111. Salpeter, E. 1955 *Astrophys. J.*, **121** 161.
112. Scalo, J. 1983 in *Protostars and Planets II*, eds. D. Black and M. S. Matthews, (University of Arizona Press: Tucson), p. 201.
113. Scalo, J. 1986 in *Fundamentals of Cosmic Phisics*, **11**, 1.
114. Scalo, J. 1990 in *Physical Processes in Fragmentation and Star Formation*, eds. R. Capuzzo-Dolcetta, C. Chiosi and A. Di Fazio (Dordrecht, Kluwer) p. 151.
115. Scalo, J. 1998 in *The Stellar Initial Mass Function*, eds. G. Gilmore and D. Howell (Astronomical Society of the Pacific, San Francisco), p.
116. Schwarzchild, M. 1958 *Structure and Evolution of Stars*, (Princeton University Press: Princeton).
117. Shu, F.H., Adams, F.C. & Lizano, S. 1987 *Ann. Rev. Astron. Astrophys.*, **25** 23.
118. Shu, F.H., Lizano, S., Ruden, S. & Najita, J. 1988 *Astrophys. J. Letters*, **328** 19.
119. Snell, R., Loren, R, &. Planbeck, R. 1980 *Astrophys. J. Letters*, **239** 17.
120. Stahler, S.W. 1983 *Astrophys. J.*, **274** 822.
121. Strom, K.M., Strom, S.E. & Merrill, M. 1993 *Astrophys. J.*, **412** 233.

122. Tatematsu, T. *et al.*, 1993 *Astrophys. J.*, **404** 643.
123. Terebey, S. 1998 unpublished HST observations.
124. Terebey, S., Shu, F.H. & Cassen, P. 1984 *Astrophys. J.*, **286** 529.
125. Testi, L. & Sargent, A.I. 1998. *Astrophys. J. Letters*, (in press).
126. van Albada, T.S. 1985 in *Birth and Evolution of Massive Stars and Stellar Groups*, eds. H. van Woerden and W. Boland, (Reidel: Dordrecht), p. 89.
127. Walker, C.K., Lada, C.J., Maloney, P., Young, E.T., & Wilking, B.A. 1986 *Astrophys. J. Letters*, **309** 47.
128. Walker, M.F. 1956 *Astrophys. J. Suppl. Ser.*, **2** 365.
129. Walter, F. 1987 *Publ. Astron. Soc. Pacific*, **99** 31.
130. Ward-Thompson, D. *et al.* 1996 *Monthly Notices Roy. Astron. Soc.*, **314** 625.
131. Whitworth, A. 1979 *Monthly Notices Roy. Astron. Soc.*, **186** 59.
132. Wilking, B.A., Lada, C.J. & Young, E.T. 1989 *Astrophys. J.*, **340** 823.
133. Wiramihardja, S. *et al.* 1991 *Publ. Astron. Soc. Japan*, **43** 27.
134. Wooten, A. 1989 *Astrophys. J.*, **337**, 858.
135. Yuan C. & You J. 1995 Molecular Clouds and Star Formation, (World Scientific, Singapore).
136. Zhou, S., Evans, N.J., Kompe, C. & Walmsley, C.M. 1993 *Astrophys. J.*, **404** 232.
137. Zinnecker, H., McCaughrean, M. & Wilking, B.A. 1993 in *Protostars and Planets III*, eds. G. Levy and J. Lunine, (University of Arizona Press, Tucson) p. 429.
138. Zuckerman, B. and Evans, N. 1974 *Astrophys. J. Letters*, **187** 67.